HHS Public Access

Author manuscript

Dev Biol. Author manuscript; available in PMC 2018 May 11.

Published in final edited form as:

Dev Biol. 2017 October 01; 430(1): 113–128. doi:10.1016/j.ydbio.2017.08.008.

BMP2 expression in the endocardial lineage is required for AV endocardial cushion maturation and remodeling

Jacob G. Saxon[a,e,1], **Daniel R. Baer**[a,1], **Julie A. Barton**[a,e,1], **Travis Hawkins**[a,e,1], **Bingruo Wu**[c], **Thomas C. Trusk**[a], **Stephen E. Harris**[b], **Bin Zhou**[c], **Yuji Mishina**[d], and **Yukiko Sugi**[a,*]

[a]Department of Regenerative Medicine and Cell Biology and Cardiovascular Developmental Biology Center, Medical University of South Carolina, Charleston, SC 29425, USA

[b]Department of Periodontics, University of Texas Health Science Center at San Antonio, San Antonio, TX 78229, USA

[c]Department of Genetics, Pediatrics and Medicine, Albert Einstein College of Medicine of Yeshiva University, Bronx, NY 10461, USA

[d]Department of Biologic and Material Sciences, School of Dentistry, University of Michigan, Ann Arbor, MI 48109, USA

[e]College of Charleston, Honors College, Undergraduate Student. Charleston, SC 29425, USA

Abstract

Distal outgrowth, maturation and remodeling of the endocardial cushion mesenchyme in the atrioventricular (AV) canal are the essential morphogenetic events during four-chambered heart formation. Mesenchymalized AV endocardial cushions give rise to the AV valves and the membranous ventricular septum (VS). Failure of these processes results in several human congenital heart defects. Despite this clinical relevance, the mechanisms governing how mesenchymalized AV endocardial cushions mature and remodel into the membranous VS and AV valves have only begun to be elucidated. The role of BMP signaling in the myocardial and secondary heart forming lineage has been well studied; however, little is known about the role of BMP2 expression in the endocardial lineage. To fill this knowledge gap, we generated *Bmp2* endocardial lineage-specific conditional knockouts (referred to as *Bmp2 cKO*^{Endo}) by crossing conditionally-targeted *Bmp2*$^{flox/flox}$ mice with a Cre-driver line, *Nfatc1*^{Cre}, wherein Cre-mediated recombination was restricted to the endocardial cells and their mesenchymal progeny. *Bmp2 cKO*^{Endo} mouse embryos did not exhibit failure or delay in the initial AV endocardial cushion formation at embryonic day (ED) 9.5–11.5; however, significant reductions in AV cushion size were detected in *Bmp2 cKO*^{Endo} mouse embryos when compared to control embryos at ED13.5 and ED16.5. Moreover, deletion of *Bmp2* from the endocardial lineage consistently resulted in membranous ventricular septal defects (VSDs), and mitral valve deficiencies, as evidenced by the

*Correspondence to: Department of Regenerative Medicine and Cell Biology, Medical University of South Carolina, 173 Ashley Avenue, BSB Rm. 635, Charleston SC 29425, USA. Fax: +1 843 792 0664. sugiy@musc.edu (Y. Sugi).

[1]Contributed equally

Author contributions

Conceived and designed the experiments: YS. Performed the experiments: JGS, DRB, TH, JAB, BW, YS. Analyzed the data: YS, DRB, JGS, TCT. Contributed reagents/materials: SHE, BZ, YM. Wrote the paper: YS, YM, TCT.

absence of stratification of mitral valves at birth. Muscular VSDs were not found in *Bmp2 cKO*^{Endo} mouse hearts. To understand the underlying morphogenetic mechanisms leading to a decrease in cushion size, cell proliferation and cell death were examined for AV endocardial cushions. Phospho-histone H3 analyses for cell proliferation and TUNEL assays for apoptotic cell death did not reveal significant differences between control and *Bmp2 cKO*^{Endo} in AV endocardial cushions. However, mRNA expression of the extracellular matrix components, *versican*, *Has2*, *collagen 9a1,* and *periostin* was significantly reduced in *Bmp2 cKO*^{Endo} AV cushions. Expression of transcription factors implicated in the cardiac valvulogenesis, *Snail2*, *Twist1* and *Sox9,* was also significantly reduced in *Bmp2 cKO*^{Endo} AV cushions. These data provide evidence that BMP2 expression in the endocardial lineage is essential for the distal outgrowth, maturation and remodeling of AV endocardial cushions into the normal membranous VS and the stratified AV valves.

Keywords

Atrioventricular cushion; BMP signaling; Endocardial lineage; Membranous ventricular septum; Heart valves; Development

1. Introduction

Valvuloseptal defects are among the most common and serious of congenital heart defects (CHDs) (Loffredo, 2000). In the atrioventricular (AV) canal, endocardial endothelial cells trans-differentiate into mesenchymal cells that populate into acellular AV endocardial cushions. Mesenchymalized AV endocardial cushions undergo distal outgrowth, maturation and remodeling into the membranous ventricular septum (VS) and the tricuspid and mitral AV valves (Review: Eisenberg and Markwald, 1995; Anderson *et al.*, 2014; de Vlaming *et al.*, 2012). The failure of these processes is thought to result in several human CHDs. Among them, membranous ventricular septal defects (VSDs) are the most prevalent human VSDs, comprising 75–80% of all VSDs (McCarty *et al.*, 2000). Despite the clinical relevance, the mechanisms governing how mesenchymalized AV cushions mature and remodel into normal valvuloseptal tissues have only begun to be elucidated.

Bone morphogenetic proteins (BMPs) are multifaceted regulators for cellular differentiation. BMPs function via cognate Type I and Type II receptors (Miyazono *et al.*, 2010). BMP signaling is critical for various aspects of cardiac development and morphogenesis (Review: Wang *et al.*, 2011). The role of BMP signaling in the myocardial and secondary heart field lineages has been extensively studied (Review: Wang *et al.*, 2011; Bai *et al.*, 2013; Briggs *et al.*, 2013; Jiao, K. *et al.*, 2003; Ma *et al.*, 2005;McCulley *et al.*, 2008;Thomas *et al.*, 2014). However, the role of *Bmp2* expression in the endocardial cells and endocardial progeny cushion mesenchymal cells has received little attention.

Bmp2 conventional knockout mice die by ED 8.5 (Zhang and Bradley, 1996) before the initial heart tube formation, which has hampered investigating the role of *Bmp2* in the cardiac development. Moreover, because myocardial *Bmp2* conditional knockout (cKO) mice die at ED 10.5 (Ma *et al.*, 2005; Rivera-Ferciano and Tabin, 2006) and *Bmpr1a* (*Alk3)* pan-endothelial cKO mice die at ED11.5 (Ma *et al.*, 2005; Song *et al.*, 2007; Park *et al.*,

2006) at the endocardial-mesenchymal transformation (EMT) stage, the role of BMP2 signaling after EMT in the AV endocardial cushions cannot be investigated using these models. *Bmp2* mRNA (Abdelwahid *et al.*, 2001), BMP2 protein (Sugi *et. al.*, 2004) and BMP type I receptors, *Bmpr1a* and *Acvr1 (Alk2)* (Desgrosellier *et al.*, 2005; Inai *et* al., 2008; Wang *et al.*, 2005) are expressed in the AV endocardium and cushion mesenchyme at and after EMT stage. Based on the expression patterns of BMP ligands and their receptors, we hypothesized that autocrine BMP signaling within endocardium and progeny endocardial cushions regulates the maturation and remodeling of mesenchymalized AV cushions after-EMT (Sugi *et al.*, 2016). The Cre driver $Nfatc1^{Cre}$, which confers Cre-mediated recombination in endocardial cells and their progeny (Wu *et al.*, 2012), has enabled us to elucidate BMP signaling mechanisms in the endocardial lineage.

The requirement of *Bmp2* expression in the myocardium (Ma *et al.*, 2005; Luna-Zurita *et al.*, 2010) and the regulation of myocardial *Bmp2* expression by the endocardium (Wang *et al.*, 2013) have been well documented for the initiation of AV endocardial cushion formation. In this work, we have studied the role of *Bmp2* expression in the endocardial lineage by generating $Nfatc1^{Cre}; Bmp2^{flox/-}$ mouse embryos (or mice). Deletion of *Bmp2* from the endocardial lineage consistently resulted in membranous VSDs, and mitral valve dysplasia which was evidenced by the absence of stratification of mitral valves at birth, indicating that BMP2 expression in the endocardial lineage is required for AV endocardial cushion maturation and remodeling into the normal membranous VS and the stratified AV valves.

2. Materials and methods

2.1. Mouse lines

Generation of *Bmp2* floxed mice ($Bmp2^{tm1Ym}$) has been described elsewhere (Singh *et al.*, 2008). The neo resistant cassette was removed from the targeted locus to avoid phenotypes caused by hypomorphic functions caused by the cassette (Singh *et al.*, 2008; Yang *et al.*, 2013). B6;129S4-$Bmp2^{tm1Jfm}$/J ($Bmp2^{floxneo}$) mice (Ma and Martin, 2005) were also used to confirm that two independently generated conditional *Bmp2* alleles resulted in the same phenotype (See *Results 3.4*). In these targeted mice, presence of the neo resistant cassette does not compromise gene function (Ma and Martin, 2005). Generation of $Nfatc1^{Cre}$ mice has been described elsewhere (Wu *et al.*, 2012). B6.129S4-$Gt\ (ROSA)\ 26Sor^{tm1Sor}$/J (*R26R*) reporter mice (Jax #0034741), and $Gt(ROSA)26Sor^{tm4\ (ACTB\text{-}tdTomato,\ \text{-}EGFP)\ Luo}$/J ($ROSA26^{mTmG}$) reporter mice (Jax #00756) were purchased from Jackson laboratory. Generation of $Bmp2^{+/-}$, *R26R,* and $ROSA26^{mTmG}$ mice has been described elsewhere, respectively (Zhan and Bradley,1996; Soriano,1999; Muzumdar *et al.*, 2007). To produce *Bmp2* conditional knockout mice for the endocardial lineage, $Nfatc1^{Cre}; Bmp2^{flox/-}$ (referred to as $Bmp2\ cKO^{Endo}$) were generated by using the breeding strategy shown in Supplementary Fig. 1. For the final crossing, $Nfatc1^{Cre};Bmp2^{+/-}$ males were bred with $Bmp2^{flox/flox}$ females to avoid potential reduction of maternal BMP2. In some cases, $Bmp2^{flox/flox}$; *R26R* double homozygous females or $Bmp2^{flox/flox}$; $ROSA26^{mTmG}$ double homozygous females were used instead of $Bmp2^{flox/flox}$ females. For genotyping, DNA was extracted from the yolk sacs or tails of mouse embryos and the tails or ears of mice afterbirth, respectively.

All experiments involving mice were carried out under our protocol (#2765) reviewed and approved by the Medical University of South Carolina Institutional Animal Care and Use Committee (IACUC) in adherence to the NIH guidelines. Noontime on the day of detecting vaginal plugs was designated as embryonic day (ED) 0.5.

2.2. General Histological analysis

Hearts from *Bmp2 cKO*^{Endo} mouse embryos and postnatal mice were processed for general histology, whole mount LacZ staining and immunohistochemical analysis as described below and compared with control (*Bmp2*$^{flox/+}$) littermate hearts.

For general histological analysis, ED8.5–13.5 mouse embryos and ED14.5–18.5 and postnatal day (PD) 1–6 mouse hearts were fixed with either 4% paraformaldehyde in phosphate buffered saline (PBS, pH. 7.4) or cold 100% methanol, depending on procedural necessity.

2.3. Whole mount β-galactosidase (LacZ) staining

ED8.5–13.5 mouse embryos and hearts from ED14.5–18.5 and postnatal mice were fixed with 4% paraformaldehyde in PBS for 15–40 min depending on the size of the tissues. Samples were rinsed overnight with 0.02% sodium deoxycholate, 0.01% NR-40/PBS for permeabilization. Samples were treated with X-gal solution for 1–3 days at 37°C with gentle rotation to detect the presence of β-galactosidase, as previously described (Snarr *et al.*, 2007). After post-fixation with 4% paraformaldehyde, samples were rinsed and dehydrated with a series of ethanol and Xylen, and embedded in paraffin.

2.4. Immunohistochemistry and histochemical localization

Paraffin sections were rehydrated and processed for immunohistochemistry as previously described (Sugi *et al.*, 2004). For localization of Twist1, Sox9, and Snail2, a standard antigen unmasking procedure (Vector Laboratories, Inc. Burlington, CA) was performed according to the manufacturer's recommendations.

Commercially available primary antibodies, anti-Collagen Type I (Col I) (Millipore, #AB765P), anti-Collagen Type IX (Col IX) (Millipore, # MAB3304), anti-versican (Chemicon, # AB1033), anti-Twist1 (abcam, #ab50887), anti-Sox9 (Santa Cruz, #SC20095) and anti-Snail2 (abcam, #ab27568) were used according to the manufacturers' recommendations. Anti-BMP2 was kindly provided by Genetics Institute (Boston) and used as previously described (Sugi *et al.*, 2004). Anti-mouse periostin antibodies were a kind gift from Drs. Hoffman and Krug (Medical University of South Carolina) and immunohistochemistry was performed as previously described (Sugi *et al.*, 2012). For the secondary antibody, either fluorescein conjugated goat anti-mouse IgG (MP Biomedicals, #55514) or -rabbit IgG (MP Biomedicals, # 55662) was used.

Hyaluronan deposition was histochemically detected with a specific hyaluronan binding protein (HABP) by following the previously described procedure (Toole *et al.*, 2001; Inai *et al.*, 2013). Biotinylated HABP (bHABP) was purchased from Seikagaku America (East Falmouth, MA).

For all immunohistochemical and histochemical localization, sections were immunostained with MF20 (Developmental Studies Hybridoma Bank) for the myosin heavy chain followed by Rhodamine-conjugated goat anti-mouse IgG (MP Biomedicals, #55539). TO-PRO-3 (Invitrogen, #T3605) was used for nuclear staining. Stained sections were examined with a Leica SP5 confocal microscope.

2.5. Cell proliferation

Cell proliferation ratio was determined by Phospho-histone (pHistone) H3 immunohistochemistry. Paraffin sections of ED13.5 septal AV cushions (fused superior and inferior AV cushions) from *Bmp2 cKO*^{Endo} and control mice were subjected to immunohistochemistry with anti-pHistone H3 (Millipore, # 06-570). All nuclei were stained with TO-PRO-3. Stained samples were observed with a Leica SP5 confocal microscope and photographs were used for quantitative analysis by analyzing 500 cells/sample collected from 4–5 frontal sections of the AV septal cushions spaced 24μm apart for 5 samples each of *Bmp2 cKO*^{Endo} and control specimens.

2.6. Apoptosis

The TUNEL assay was performed to detect cell death in AV septal cushions. Paraffin sections from ED13.5 AV septal cushions from *Bmp2 cKO*^{Endo} and control mice were subjected to the TUNEL assay using In the Situ Cell Death Detection Kit, Fluorescein (Roche, # 1168479591). All nuclei were stained with TO-PRO-3. Stained samples were observed with a Leica SP5 confocal microscope and photographs were used for quantitative analysis by analyzing 500 cells/sample collected from 4–5 frontal sections of the AV septal cushions spaced 24μm apart for 5 samples each of *Bmp2 cKO*^{Endo} and control specimens.

2.7 Cell Density

Cell density was analyzed at ED13.5 in paraffin sections of septal AV cushions from *Bmp2 cKO*^{Endo} and control mouse embryos. Nuclei were stained with TO-PRO-3. Stained samples were observed with a Leica SP5 confocal microscope and photographs were used for quantitative analysis. AV cushion area was measured with ImageJ processing program and nuclei were counted manually in 5 frontal sections of the AV septal cushions spaced 24μm apart in each of 5 samples from each group. Cell density was calculated as the number of nuclei divided by AV cushion area.

2.8. Amira three-dimensional (3-D) reconstruction and volumetric analysis

Amira™ software (version 6.1.1, FEI, Hillsboro, OR) was used for three-dimensional (3-D) reconstruction of septal AV endocardial cushions (fused inferior and superior AV cushions) and cardiac walls from LacZ-stained ED13.5 and ED16.5 *Nfatc1*^{Cre}*; Bmp2*$^{fx/-}$ *R26R* (*Bmp2 cKO*^{Endo}) mouse embryos and littermates, *Nfatc1*^{Cre}*; Bmp2*$^{fx/+}$ *R26R* embryos. Serial sections (6μm) were cut from LacZ-stained, paraffin-embedded samples and counter stained with eosin. Digital photographs of heart sections taken with an Olympus BX40 microscope were entered sequentially into Amira and aligned using the sum of least squares alignment algorithm. Additional alignment corrections were made visually by using the outlines of the LacZ positive septal mesenchyme as landmarks.

To assess the volumetric effects of the reduction of BMP2 in the endocardial linage for septal AV cushions, volumetric analyses were performed using 5 independent reconstructions each for the *Bmp2 cKO*^{Endo} and *Nfatc1*^{Cre}*; Bmp2*$^{fx/+}$ mice from two sets of ED13.5 and ED16.5 litters. Results at each stage were compared using a two-tailed Student's t-test.

2.9. Quantitation of valve thickness

The thickness of the widest portion of the anterior (septal) leaflets of mitral valves was measured at PO5 in paraffin sections from *Bmp2 cKO*^{Endo} and control mouse hearts. Using ImageJ, 3 measurements per leaflet in 7–10 frontal sections spaced 36μm apart in each were taken in 5 samples from each group.

2.10. Quantitative RT-PCR

RNA extraction was performed on two-three pooled septal portions of AV canals from two-three litters each of ED13.5 *Bmp2 cKO*^{Endo} and control mouse embryos. Because ECM components and transcription factors examined in this work are predominantly localized in the cushion mesenchyme but not in the associated myocardium, the results obtained from the quantitative RT-PCR are expected to represent their expression in the cushion mesenchyme. Reverse transcription and real-Time PCR were performed as described previously for AV cushion mesenchymal cells (Inai et al., 2008; 2013). Briefly, total RNA was extracted with RNA STAT- 60 (Tel-Test. Inc) and purified using the Arcuturus™ PicoPure™ RNA Isolation Kit (Applied Biosystems). Complementary DNA was prepared by using the iScript cDNA synthesis kit (Bio-Rad) according to the manufacturer's recommendations. Real time PCR was performed using SsoAdvanced Universal SYBR Green Supermix with the Bio-Rad CFX96 Real-Time PCR detection system (Bio-Rad). PCR primers used for the quantitative RT-PCR (qRT-PCR) in this study are listed in the Supplementary Table 1. Amplification of each listed genes were normalized to mouse *β-actin* amplification. No-reverse transcription controls were included in each reaction. Melting curve analysis indicating a single peak was performed to confirm that the PCR reaction was specific for each gene of interest. Quantification was performed using the relative standard curve method; controls were assigned a value of 1 and experimental values were calculated based on the C_T values, relative to the control standard curve. qRT-PCR results represent at least three independent RNA samples, with each reaction performed in triplicate.

2.11. Collagen gel assay for endocardial cushion mesenchymal cell formation

The preparation of hydrated collagen gels was essentially the same as described previously (Sugi *et al.*, 2004). The AV regions of hearts were dissected out from ED9.5 mouse embryos. Each AV region was cut longitudinally to expose the lumen and placed on the hydrated and drained collagen gels (1mg/ml, type I rat-tail tendon collagen, BD Biosciences) that had been saturated with OptiMEM medium (Invitrogen) supplemented with 1% heat-inactivated fetal bovine serum (Hyclone), ITS (5 μg/ml insulin, 5 μg/ml transferrin, 5ng/ml selenium, BD Biosciences), and streptomycin/penicillin (Invitrogen). Media were added to the culture 2 hours after placement of AV explants. Mesenchymal formation was assessed by counting the number of mesenchymal cells that migrated out from the explants with an inverted microscope (Leica DMIRB) with Hoffman optics. Cell numbers were normalized by

measuring the area of the each explant from photographs with Amira™ software as previously described (Harikrishnan *et al.*, 2015).

2.12. Statistical analyses

Statistical data are presented as the mean ± standard error of the mean (SEM). For the quantitative analyses, mean values were compared using a two-tailed Student's t-test to determine if each difference was statistically significant. Differences were considered significant if $p<0.05$.

3. Results

3.1. Nfatc1^{Cre}-mediated recombination is restricted to endocardial cells and their transformed progeny mesenchymal cells

Whole mount LacZ staining showed endocardial-specific Cre-mediated recombination specifically in hearts from ED9.5 to ED11.5 (Fig. 1A–D). LacZ staining was visible as early as ED9.0 (not shown) and distinct after ED 9.5 in X-gal-treated *Nfatc1^{Cre}; R26R* mouse embryos (Fig. 1A). Recombination was restricted to endocardial cells and their transformed mesenchymal progeny (Fig. 1D). There was no detectable recombination in the vascular endothelial cells (Fig. 1D), which was consistent with the previous findings (Wu *et al.*, 2012). Importantly, proximal outflow tract (pOFT) cushions as well as superior and inferior AV cushions were populated with LacZ-positive mesenchymal cells that were derived from *Nfatc1* positive endocardium (Fig. 1D). These results indicate that the *Nfatc1^{Cre}*driver line can delete *Bmp2* specifically from endocardial cells and their progeny mesenchymal cells during early cardiac development. This notion is critical because BMP signaling is known to be required for the formation of the vascular endothelium (Cai *et al.*, 2012; Morrell *et al.*, 2016); therefore, the usage of an endocardial-specific but not pan-endothelial Cre driver line is critical for addressing the role of *Bmp2* expression exclusively in the endocardial lineage during cardiac development.

3.2. Deletion of Bmp2 from the endocardial lineage leads to early postnatal lethality

Bmp2 mRNA (Abdelwahid *et al.*, 2001) and BMP2 protein (Sugi *et al.*, 2004, also see Fig. 2 for ED13.5) are expressed in AV endocardial cushions during AV cushion maturation and remodeling. To delete *Bmp2* from endocardial lineage, including endocardial cells and endocardial progeny cushion mesenchymal cells, we generated *Bmp2* cKO^{Endo} by using the breeding strategy indicated in Supplementary Fig. 1. Deletion of *Bmp2* from the endocardial lineage led to early postnatal lethality (Fig. 3A, B). *Bmp2 cKO^{Endo}* mouse embryos survived until birth without significant loss, at the expected Mendelian frequency of 25% (Fig. 3B and Table 1). Immediately after birth, *Bmp2 cKO^{Endo}* mice began to die. *Bmp2 cKO^{Endo}* mice did not survive beyond PD6. Heterozygous deletion of *Bmp2* (*Bmp2$^{+/-}$*) did not affect survival rate (Table 1). *Bmp2$^{+/-}$* mice were viable and did not exhibit cardiac defects in consistence with the previous observations (Goldman *et al.*, 2009; Uchimura *et al.*, 2009). These data indicate that *Bmp2* in the endocardial lineage plays critical roles in the survival of *Bmp2* cKO^{Endo} mice after birth.

3.3. Deletion of Bmp2 from the endocardial lineage does not affect initial AV endocardial cushion formation

Endocardial cushion mesenchymal cells are formed through endocardial epithelial-mesenchymal transformation (EMT) (Armstrong and Bischoff, 2004; Combs and Yutzey, 2009; Eisenberg and Markwald, 1995; Person *et al.*, 2005). Mesenchymal cell formation commences in the AV and outflow tract at around ED9.5 and ED10.5, respectively in mice (Camenisch *et al.*, 2002; Sugi *et al.*, 2004). Myocardial deletion of *Bmp2* leads to formation of hypoplastic AV cushions at ED9.5 and embryonic lethality at ED10.5 (Ma *et al.*, 2005; Rivera-Ferciano and Tabin, 2006). However, *Bmp2 cKO*^{Endo} mouse embryos were indistinguishable from control littermates at ED9.5 and10.5 by morphological analyses (not shown). Moreover, EMT assays using collagen gel cultures did not reveal any delay or reduction of mesenchymal cell formation from *Bmp2 cKO*^{Endo} AV explants that were cultured in the presence of adjacent AV myocardium (Fig. 4A–C). By ED11.5, fully developed superior and inferior AV cushions were observed in the AV canal in control mouse embryos (Fig. 4D). We compared AV endocardial cushions in *Bmp2 cKO*^{Endo} (*Nfatc1*^{Cre}; *Bmp2*$^{flox/-}$) mouse embryos with those in littermate control (*Bmp2*$^{flox/+}$), conventional BMP2 heterozygous (*Bmp2*$^{flox/-}$), and endocardial lineage-specific BMP2 heterozygous (*Nfatc1*^{Cre}; *Bmp2*$^{flox/+}$) mouse embryos (Fig. 4D–G). Histological analysis did not reveal any discernible abnormalities in AV endocardial cushions of *Bmp2 cKO*^{Endo} or conventional and endocardial lineage specific *Bmp2* heterozygous mouse embryos as compared to control embryos at ED11.5 (Fig. 4D–G). These results indicate that deletion of *Bmp2* from the endocardial lineage do not either delay or reduce initial formation of AV endocardial cushions, suggesting that myocardially expressed *Bmp2* is sufficient for initial cushion formation through EMT, and indicating that *Bmp2* expression in the endocardial lineage is dispensable for the initial formation of AV endocardial cushions.

3.4. Deletion of Bmp2 from the endocardial lineage consistently results in (peri)-membranous ventricular septal defects (VSDs)

Histological analysis revealed that *Bmp2 cKO*^{Endo} mouse embryos consistently exhibited membranous VSDs at ED15.5/16.5 with nearly complete penetrance (92%, n=13) (Fig. 5B, D). By ED15.5/16.5, control mouse embryos showed fully formed membranous VS that was filled with Alcian Blue-positive, glycosaminoglycan-enriched extracellular matrix (ECM) (Fig. 5A, C), whereas *Bmp2 cKO*^{Endo} mouse embryos exhibited loss or significant reduction of Alcian Blue-positive, glycosaminoglycan enriched-ECM (Fig. 5D). Membranous VSDs observed in *Bmp2 cKO*^{Endo} mouse embryos were isolated and other significant cardiac defects such as atria septal defects (ASD), myocardial VSDs, double outlet right ventricle (DORV), or persistent truncus arteriosus (PTA) were not found in *Bmp2 cKO*^{Endo} mouse embryos. Tissue examination of lung, liver and pancreas after birth did not reveal discernible defects (not shown). Although 92% (n=13) of *Bmp2 cKO*^{Endo} mouse embryos exhibited membranous VSDs at ED15.5/16.5, *Bmp2 cKO*^{Endo} embryos were recovered at normal Mendelian frequencies of 25% until birth (Table 1), suggesting that maternal blood flow supported survival of the embryos. Many of the most severely affected *Bmp2 cKO*^{Endo} newborn mice were lost immediately after birth and some of them were not able to be morphologically analyzed; however, all *Bmp2 cKO*^{Endo} newborn mice that were obtained and analyzed showed membranous VSDs (n=5, Supplementary Fig. 2). Myocardial

deficiencies, such as muscular VSDs, were not evident in the *Bmp2 cKO*^{Endo} mouse embryos (Fig. 5B, D). Control, *Bmp2* heterozygous and *Bmp2* endocardial lineage specific heterozygous deletion did not reveal any cardiac defects including membranous VSDs at ED15.5/16.5, consistent with previous findings with *Bmp2* heterozygous knockout mice (Goldman *et al.*, 2009; Uchimura *et al.*, 2009). We further examined the independently generated conditional mouse line for *Bmp2* (Ma and Martin, 2005) for comparison. Resulted *Nfatc1*^{Cre}; *Bmp2*$^{floxneo/-}$ mouse embryos consistently showed the same phenotypes, i. e., membranous VSDs at ED15.5/16.5 (Supplementary Fig. 3). Taken together, our data indicate that *Bmp2* expression in the endocardial lineage is required for proper formation of the membranous VS.

3.5. Three-dimensional (3-D) reconstruction and volumetric analysis reveal that the reduction of Bmp2 from the endocardial lineage results in a decrease of AV endocardial cushion size as early as ED13.5

Superior and inferior AV cushions fuse to form a septal AV cushion in the middle of the AV canal by ED13.5 in mouse embryos (Anderson *et al.*, 2014). To find the effect of reducing *Bmp2* within the endocardial linage, septal AV endocardial cushions in *Bmp2 cKO*^{Endo} (*Nfatc1*^{Cre}*; Bmp2*$^{flox/-}$*; R26R*) mouse embryos were compared with those in littermates *Nfatc1*^{Cre}*; Bmp2*$^{flox/+}$*; R26R* mouse embryos. Specifically in this experiment, LacZ-positive septal AV cushions and their derivative, membranous VS were traced for 3D reconstruction. Fusion of the superior and inferior AV endocardial cushions commenced at ED12.5 in control *Nfatc1*^{Cre}*; Bmp2*$^{flox/+}$*; R26R* mouse embryos. Although there was a slight delay in fusion of AV endocardial cushions in *Bmp2 cKO*^{Endo} (*Nfatc1*^{Cre}*; Bmp2*$^{flox/-}$*; R26R*) mouse embryos when compared to controls (data not shown), the majority of the central portion of the superior and inferior AV endocardial cushions were fused in both *Nfatc1*^{Cre}*; Bmp2*$^{flox/+}$*; R26R* and *Bmp2 cKO*^{Endo} mouse embryos by ED 13.5. 3D reconstruction and volumetric analysis revealed significant reductions in the size of fused septal AV cushions at ED13.5 in *Bmp2 cKO*^{Endo} mouse embryos as compared to those in control mouse embryos (Fig. 6A–G). At ED16.5, 3D reconstruction and volumetric analysis revealed loss of the central portion of the membranous VS and significant reductions in the size of the membranous VS in *Bmp2 cKO*^{Endo} embryos as compared to control mouse embryos (Fig. 6H–N). These data indicate that reducing *Bmp2* within the endocardial lineage significantly decreases the size of AV endocardial cushions and suggest that the reduction of AV endocardial cushion size results in loss of membranous VS.

3.6. Cell proliferation and cell death are not significantly affected by deletion of Bmp2 from the endocardial lineage

To examine whether changes in proliferation and/or apoptosis were the underlying morphogenetic mechanisms leading to the decrease of endocardial cushion size, proliferation and apoptotic cell death were examined in *Bmp2 cKO*^{Endo} and control septal AV cushions at ED13.5. Phospho-histone (pHistone) H3 immunohistochemistry was performed to analyze cell proliferation in AV endocardial cushions (Fig. 7A–C). A slight reduction of pHistone H3-positive cell numbers was observed; however, there was no statistically significant decrease of cell proliferation in septal AV cushions in *Bmp2 cKO*^{Endo} mouse embryos as compared to controls ($p=0.67$). As determined by TUNEL assay, there

was no significant change in apoptotic cell death ratio in the septal AV cushions of *Bmp2 cKO^{Endo}* mouse hearts as compared to controls (*p=0.84*) (Fig. 7D–F).

We further examined cell density in the septal AV cushions at ED13.5 (Fig. 8). *Bmp2 cKO^{Endo}* mouse AV endocardial cushions showed a significant increase in cell density (Fig. 8C). Size of the AV endocardial cushion was reduced in the *Bmp2 cKO^{Endo}* mouse embryos at ED13.5 (Fig. 6G). Therefore, an increase of cell density in *Bmp2 cKO^{Endo}* mouse embryos is consistent with the idea that cell number in the endocardial cushion is not significantly reduced. Taken together, these data provide supportive evidence that cell proliferation and apoptosis did not critically associated with the decrease of AV endocardial cushion size.

To determine whether insufficient growth of the muscular portion of the ventricular septum (muscular VS) contributed to the membranous VSDs observed in *Bmp2 cKO^{Endo}* mouse embryos, proliferation and apoptotic cell death were examined in *Bmp2 cKO^{Endo}* and control muscular VS at ED13.5 (Supplementary Fig. 5). There were no significant changes in cell proliferation (*p=0.45*) or apoptotic cell death ratio (*p=0.56*) in the muscular VS of *Bmp2 cKO^{Endo}* mouse hearts as compared to controls (Supplementary Fig. 5C, F). These data provide supportive evidence that insufficient growth of the muscular VS is not associated with the decrease of AV endocardial cushion size and membranous VSDs found in *Bmp2 cKO^{Endo}* mice.

3.7. Expression of Proteoglycans and a matricellular protein, periostin is reduced by deletion of Bmp2 from the endocardial lineage

To examine whether changes in the expression of ECM components, versican, hyaluronan and matricellular protein, periostin were associated with the decrease of endocardial cushion size, quantitative RT-PCR was performed for the septal portions of AV canals in *Bmp2 cKO^{Endo}* and control mouse embryos at ED13.5. ECM components, versican, hyaluronan and periostin were localized in the septal AV cushions of control and *Bmp2 cKO^{Endo}* mouse embryos at ED13.5 (Fig. 9A, B, E, G, H). Hyaluronan synthase 2 (*Has2*) is the only known *Has* responsible for hyaluronan (HA) production in the heart (Camenisch *et al.*, 2000). Therefore, *Has2* mRNA expression was used as an index of HA production. Quantitative RT-PCR revealed that the mRNA expression of *versican*, *Has2* and *periostin* was significantly reduced (*p<0.05*) in *Bmp2 cKO^{Endo}* mouse AV canals as compared to controls (Fig. 9. C, F, I). These data indicate that decreases in expression of these ECM components are associated with a decrease in size of AV endocardial cushions in *Bmp2 cKO^{Endo}* mouse embryos.

3.8. Expression of Col9a1 is reduced by deletion of Bmp2 from the endocardial lineage

To examine whether changes in the expression of ECM components *Col1a1* or *Col 9a1* were associated with the decrease of endocardial cushion size, qRT-PCR was performed for the septal portions of AV canals in *Bmp2 cKO^{Endo}* and control mouse embryos at ED13.5. Col I and Col IX proteins were localized in the septal AV cushions of control and *Bmp2 cKO^{Endo}* mouse embryos at ED13.5 (Fig. 10A, B, D, F). Quantitative RT-PCR revealed that mRNA expression of *Col9a1* was significantly reduced (*p<0.05*) in the *Bmp2 cKO^{Endo}* mouse AV canals as compared to controls (Fig. 10F). *Col1a1* expression was slightly reduced; however

a statistically significant decrease of *Col1a1* was not evident in the AV canal (Fig. 10C). These data indicate that the reduction of *Col9a1* expression is associated with a decrease in size of AV cushions in *Bmp2 cKO*^{Endo} mouse embryos. Taken together, these data provide evidence that *Bmp2* expression in the endocardial lineage is required for the proper expression of ECM components and suggest that decreases in expression of these ECM components can be the one of the underlying mechanisms that leads to a decrease in size of AV endocardial cushions in *Bmp2 cKO*^{Endo} mouse embryos.

3.9. Expression of cardiac transcription factors, Twist1, Sox9 and Snail2 is reduced in the AV canal of Bmp2 cKO^{Endo} mouse embryo hearts

To further explore the underlying mechanisms of the reduction of AV endocardial cushion size, expression levels of transcription factors that are known to be expressed and potentially regulated by BMP signaling pathways in the hearts were analyzed by qRT-PCR for the septal portions of AV canals in *Bmp2 cKO*^{Endo} and control mouse embryos at ED13.5. Twist1, Sox9 and Snail2 were localized in the septal AV cushions of control and *Bmp2 cKO*^{Endo} mouse embryos at ED13.5 (Fig. 11A, B, D, E, G, H). Significant reductions in the mRNA expression of *Twist1*, *Sox9* and *Snail2* were detected in the AV canal of *Bmp2 cKO*^{Endo} mouse embryos as compared to controls (Fig. 11C, F, I). These data indicate that deletion of *Bmp2* from the endocardial lineage lead to significant reductions of the cardiac transcription factors, *Twist1*, *Sox9* and *Snail2*, providing evidence that *Bmp2* expression in the endocardial lineage is required for the normal expression of *Twist1*, *Sox9* and *Snail2* in the septal AV cushions.

3.10. *Bmp2 cKO*^{Endo} mice exhibit mitral valve dysplasia and loss of stratification

Mitral valve defects were not clearly evident at ED18.5 (not shown) but became prominent afterbirth in *Bmp2 cKO*^{Endo} mice (Figs. 12 and 13, Supplementary Fig. 4). Tricuspid valves, on the other hand, did not exhibit discernible abnormalities (supplementary Fig. 4B). Presumably due to the presence of BMP4 in the outflow tract (OFT) (Bai *et al.*, 2013), significant defects were not found in the OFT valves (not shown). More distinct defects were observed in the septal (aortic) leaflets than the left parietal (mural) leaflets of the mitral valves. *Bmp2 cKO*^{Endo} mice showed variable severity of mitral valve phenotypes. Some of the most severely affected *Bmp2 cKO*^{Endo} mice exhibited enlarged septal (aortic) leaflets of mitral valves (Supplementary Fig. 4); however, statistical analysis did not reveal a significant increase in the mitral valve thickness from moderately affected *Bmp2 cKO*^{Endo} mice at PD5 (Supplementary Fig. 6).

Normal human mitral valves are stratified into three well-defined tissue layers--the atrialis, spongiosa and fibrosa/ventricularis (Review: Levine *et al.*, 2015, Lincoln and Garg, 2014). In mice, the ECM stratification is less prominent; however, we found two identifiable layers; the fibrosa with a dense fibrous layer of collagens and the thicker spongiosa which is enriched with proteoglycans in the neonatal mouse mitral valves. To examine whether the stratification remained normal, immunohistochemistry was performed to localize proteoglycans, versican and hyaluronan (Fig. 12A–D), and Collagens, Col I and Col X, and a matricellular protein, periostin (Fig. 13A–F) in control and *Bmp2 cKO*^{Endo} mitral valves at PD5. Versican and hyaluronan were intensely deposited in the spongiosa in control valves

(Fig. 12A, C); however, *Bmp2 cKO*^{Endo} valves exhibited loss of stratification and showed expansion of the spogiosa (Fig. 12B, D). Col I and Col IX were intensely expressed in the fibrosa of control mitral valves (Fig. 13A, C), whereas dispersed expression of Col IX and Col I was seen in the expanded spongiosa of *Bmp2 cKO*^{Endo} mitral valves (Fig. 13B, D). Periostin appeared deposited in the fibrosa in a pattern similar to that of collagen deposition in the control (Fig. 13E) but was found entirely dispersed in the enlarged valve leaflets (Fig. 13F). Loss of stratification in the septal (aortic) leaflets of mitral valves was seen all *Bmp2 cKO*^{Endo} mice we examined regardless of the severity of valve phenotypes (n=6). Taken together, these data lead us to conclude that BMP2 expression in the endocardial lineage during embryonic valvulogenesis plays critical roles for the normal stratification of mitral valves after birth.

4. Discussion

Requirement of *Bmp2* expression by the myocardium (Ma *et al.*, 2005) and the importance of a endocardial-myocardial interaction (Wang *et al.*, 2013) have been demonstrated for the initial AV cushion formation. In this work, we studied the role of BMP2 expressed in the AV endocardial cells and endocardial progeny cushion mesenchymal cells by deleting *Bmp2* specifically from the endocardial lineage using the *Nfatc1*^{Cre} driver line. Deletion of *Bmp2* from the endocardial lineage did not delay or reduce the initial formation of AV endocardial cushions, suggesting that myocardial expression of BMP2 is sufficient for initial cushion formation through EMT. Expression of *Bmp2* and BMP2 is restricted to the AV canal myocardium before and during initial endocardial cushion formation (-ED11.5); however, myocardial *Bmp2*/BMP2 expression is diminished after ED11.5 (Sugi *et al.*, 2004; Ma *et al.*, 2005). On the contrary, *Bmp2* (Abdelwahid *et al.*, 2001) and BMP2 (Sugi *et al.*, 2004) are expressed in the AV endocardial cushions during the maturation/remodeling stage at ED13.5. In addition, as seen in Figs. 6–10, septal AV endocardial cushions become structurally distant from parietal AV canal myocardium by ED13.5. These spatial and temporal expression patterns may explain why BMP2 expression in the endocardial lineage is not required for the initial formation of AV endocardial cushions but is essential for their later maturation and remodeling. Our data revealed that BMP2 expression in the endocardial lineage is essential for the formation of the membranous ventricular septum and the stratified mitral valves, indicating that BMP2 expression in the endocardial lineage is required for proper AV endocardial cushion maturation and remodeling.

There are four AV cushions formed in the AV canal. In the AV canal of mice, superior and inferior AV cushions are formed first, at around ED 9.0–9.5, and much smaller right and left lateral cushions are formed later, at around ED 12.5. After endocardial endothelial cells trans-differentiate into cushion mesenchymal cells which populate into acellular AV cushions, mesenchymalized AV endocardial cushions fuse, mature and remodel into the membranous ventricular septum and the tricuspid and mitral AV valves (Review: Eisenberg and Markwald, 1995). Septation of the AV canal is the essential morphogenetic event for four-chambered heart formation. Secondary heart field derived dorsal mesenchymal protrusion (DMP) (Snarr *et al.*, 2007), also called spina vestibuli (Tasaka *et al.*, 1996), or vestibular spine (Webb *et al.*, 1998), forms an essential component of the AV septal complex in which fused AV endocardial cushions (septal AV cushions) make the major contributions

(Snarr *et al.*, 2008). Several recent papers have shown that DMP defects result in primary atrial septal defects (pASD) or incomplete AV septal defects (AVSDs), indicating the critical roles of DMP in AV septal morphogenesis (Review: Burns *et al.*, 2016). On the other hand, AV endocardial cushions have been documented to form the primordia of the membranous atrioventricular/ventricular septum and therefore, AV endocardial cushions are the structures that close embryonic interventricular communication (Anderson *et al.*, 2014). In the present work, by using *Nfatc1*^{Cre}-mediated endocardial lineage tracing, we provide evidence that the membranous VS is indeed derived from AV endocardial cushions (Fig. 6). Moreover, we demonstrate that endocardial lineage-specific deletion of *Bmp2* results in significant reductions in the AV cushion volume and causes membranous VSDs in mice (Figs. 5, 6). Our data indicate that regulation of AV endocardial cushion growth by BMP2 expression in the endocardial lineage is crucial for membranous VS formation. Regarding the significance of the membranous VSDs that comprise 75–80% of human VSDs (McCarthy *et al.*, 2000), there is no doubt that AV endocardial cushions play an essential and indispensable role in four-chambered heart formation.

Bmp2 and *Bmp4* genes are highly conserved with over 90% similarity between the mature proteins. Previous work using conventional compound heterozygous mice for *Bmp2* and *Bmp4* has revealed several morphogenetic failures including VSDs and abnormalities in the AV valve leaflets of the compound heterozygous hearts (Goldman *et al.*, 2009; Uchimura *et al.*, 2009). Although the half of the compound heterozygous mice dies soon after birth, mice lacking a single copy of *Bmp2* or *Bmp4* are viable and have little cardiac defects (Goldman *et al.*, 2009; Uchimura *et al.*, 2009). Consistent with these findings, we did not observe cardiac defects, such as AV endocardial cushion defects in heterozygous mutant mice for a null allele of *Bmp2* (*Bmp2*$^{fx/-}$) (n=6 at ED15.6/16.5). *Bmp2* heterozygous mutant mice were viable while their littermate *Bmp2* cKO^{Endo} (*Nfatc1*^{Cre}; *Bmp2* $^{flox/-}$) embryos exhibited profound defects, membranous VSDs (92% penetrance n=13 at ED15.6/16.5) and mitral valve dysplasia (n=5 afterbirth). These data indicate that the defects we observed in the *Bmp2 cKO*^{Endo} mice cannot be compensated by the presence of *Bmp4* and are specific for *Bmp2* deletion from the endocardial lineage.

ECM components are deposited in the maturing AV endocardial cushions and reported to play significant roles in valvulogenesis and valve disease development (Review: de Vlaming *et al.*, 2012; Camenisch *et al.*, 2000; Camenisch *et al.*, 2002; Dupuis *et al.*, 2011; Hinton *et al.*, 2006; Hinton and Yutzey, 2011; Lincoln *et al.*, 2006b; Norris *et al.*, 2008; Peacock *et al.*, 2008; Sugi *et al.*, 2012; Yamamura *et al.*, 1997). Furthermore, our previous work with 3-D chick AV cushion mesenchymal cell aggregate cultures has indicated that BMP2 induces mRNA expression and deposition of ECM components, periostin (Inai *et al.*, 2008), hyaluronan and versican (Inai *et al.*, 2013). Consistent with our previous findings with *in vitro* 3-D AV cushion mesenchymal cell cultures, *Bmp2 cKO*^{Endo} mouse embryos exhibited decreases in expression of *versican*, *Has2* and *periostin* in AV endocardial cushions at ED13.5 (Fig. 9). Our present work, for the first time, indicates the requirement of BMP2 expression in the endocardial lineage for ECM expression during AV cushion maturation and remodeling *in vivo*. Moreover, our present study reveals that collagen expression is decreased; specifically, there is a significant reduction of *Col9a1* in AV endocardial cushions of *Bmp2 cKO*^{Endo} mouse embryos (Fig. 10). Because cell proliferation and apoptotic cell

death are not significantly altered in the *Bmp2 cKO*^{Endo} (Fig. 7), the reduction of expression and deposition of ECM components explains the reasons why AV endocardial cushion volume is reduced as documented in Fig. 6 in the *Bmp2 cKO*^{Endo} mouse hearts. Taken together, our data provide the insight into the underlying mechanisms regulating AV cushion maturation and remodeling.

In mature cardiac valves, ECM organization is thought to be conserved across species. Developmental studies have demonstrated that ECM stratification in semilunar and AV valves begins during the late embryonic stages and continues into the postnatal stages (Aikawa *et al.*, 2006; Hinton *et al.*, 2006). Diseased valves from pediatric patients are characterized by thickened valve leaflets with increased and disorganized collagens and proteoglycans, and decreased and fragmented elastic fibers (Hinton *et al.*, 2006). In the adult human AV valve leaflets, three distinct layers are identified (Review: Levine *et al.*, 2015). During AV valve development, the endocardial cushion mesenchyme matures and remodels into stratified AV valve leaflets in human (Review: de Vlaming *et al.*, 2012). In mice, the ECM stratification is less prominent; however, we identified at least two layers, a collagen-enriched fibrosa and a proteoglycan-enriched spongiosa in neonatal mouse mitral valves (Fig. 12A, C and Fig. 13A, C, E). *Bmp2 cKO*^{Endo} mice exhibited the absence of ECM stratification, which was characterized by the expansion of the spongiosa and dispersed collagens, especially Col IX, in the fibrosa of the mitral valves (Fig. 12B, D and Fig. 13B, D, F). Although there was no statistically significant increase in valve leaflet thickness in surviving moderately affected mice (Supplementary Fig. 6), *Bmp2 cKO*^{Endo} mitral valves that lacked normal stratification structurally resembled degenerative human mitral valves (Fig. 12B, D, Fig. 13B, D, F). The structural deficiencies in *Bmp2 cKO*^{Endo} valves were not obvious during embryonic development but became prominent after birth. Dramatic changes in the circulatory system and hemodynamics at birth results in stronger sheer stress on the mitral valves. Our present data suggest that lack of BMP2 in the endocardial lineage during development renders valve interstitial cells more susceptible to the hemodynamic sheer stress, which leads to degenerative changes in the mitral valves. Our data in this study indicate that BMP2 expression in the endocardial lineage during embryonic development is essential for proper ECM remodeling and stratification and potentially prevents degenerative changes in the mitral valves.

Deletion of Type 1 BMP receptor, BMP receptor 1A, *Bmpr1a* (*Alk3*), from epicardial cells and their progeny epicardially derived parietal AV valve mesenchymal cells, is reported to result in AV valve abnormalities and myxomatous valve degeneration (Lockhart *et al.*, 2014). However, a recent paper has shown that deletion of *Bmpr1a* with a *PostnCre* (Lindsley *et al.*, 2007) mesenchymal lineage driver line do not cause aortic or mitral valve defects at PD1 (Gomez-Stallons *et al.*, 2016). In the present study, we demonstrate that *Bmp2 cKO*^{Endo} mice consistently exhibit membranous VSDs (Fig. 5, 6) and mitral valve dysplasia (Figs. 12, 13). *Bmp2 cKO*^{Endo} mouse embryos do not exhibit defects or delay in the initial endocardial cushion formation at ED11.5 (Fig. 4) and therefore, defects found in the *Bmp2 cKO*^{Endo} mice are likely derived from deficiencies in the AV cushions after EMT stage. In the AV endocardial cushions in *PostnCre; Bmpr1a*$^{flox/flox}$ mouse embryos, another Type I BMP receptor, activin receptor I, ACVR1 (ALK2), which plays an essential role in AV cushion maturation (Wang *et al.*, 2005), might compensate for the loss of BMPR1A-

mediated BMP signaling. The defects we found in the *Bmp2 cKO*^{Endo} mice can be resulted from the loss of BMP2 in the endocardium or endocardial cushion mesenchyme, as *Bmp2* and BMP2 are expressed in the AV endocardium and AV endocardial cushions during AV cushion maturation (Abdelwahid *et al.*, 2001; Sugi *et al.*, 2004). Future experiments dissecting the role of endocardial BMP2 versus endocardial cushion-expressed BMP2 might answer these intriguing questions.

In our present study, we found that expression of transcription factors, *Snail2 (Slug)*, *Sox9* and *Twist1* is significantly reduced in *Bmp2 cKO*^{Endo} mouse AV cushions (Fig. 11). *Snail2* is expressed in AV endocardial cushion cells right after mesenchymal cell formation at ED 9.5; expression continues in fused septal AV cushions and is known to induce cell migration (Niessen *et al.*, 2008). *Twist1* is also expressed in septal AV cushions during mouse development at ED13.5 (Chakraborty *et al.*, 2008;Shelton and Yutzey, 2008) but no longer detected in the ED17.5 or PD7 AV valves. *Twist1* is reported to function in cell migration and proliferation (Lee and Yutzey, 2011) and increases gene expression of ECM proteins such as the collagens, *Col1a1; Col2a1*, *Col3a1*, and periostin as well as matrix remodeling enzymes, *Mmp2* and *Mmp13* in developing AV valve leaflets (Chakraborty *et al.*, 2010). *Sox9* is another transcription factor known to be expressed in the AV endocardial cushions (Lincoln *et al.*, 2007) and shown to be required for normal deposition and organization of ECM components, such as Collagen II, cartilage link protein, tenascin and elastin (Lincoln *et al.*, 2007). *Sox9* is also known to suppress matrix mineralization (Peacock *et al.*, 2011) and regulate heart valve calcification (Peacock *et al.*, 2010). *In vitro* culture assays have shown that BMP2 can promote expression of *Twist1* (Inai *et al.*, 2008; Shelton and Yutzey; 2008) and *Sox9* (Lincoln *et al.*, 2006a). BMP4 is shown to directly target *Snail2* (*Slug*) in human embryonic stem cells (Richter *et al.*, 2013). Moreover, a recent study revealed that *Sox9* modulates other key transcription factors required for heart valve development (Garside *et al.*, 2015). In this work, by using conditionally targeted mouse models, we present for the first time that BMP2 expression in the endocardial lineage is required for the normal expression of *Snail2*, *Twist1* and *Sox9 in vivo,* suggesting that BMP2 expression in the endocardium and cushion mesenchyme plays crucial roles in AV cushion maturation and remodeling by regulating these critical transcription factors in cardiac valvuloseptal morphogenesis.

Supplementary Material

Refer to Web version on PubMed Central for supplementary material.

Acknowledgments

The authors thank Drs. Allan Bradley, Hongbing Zhan and James F. Martin for the mutant mouse line. The Authors are also grateful to the MUSC Proteogenomics Core (Dr. Jeremy Barth, Director) and Joshua Spruill Molecular Morphology Core (Dr. Thomas Trusk, Director) in the Department of Regenerative Medicine and Cell Biology (MUSC) for the usage of the facilities.

Funding sources

This work was supported by the NIH/NIGMS (P20 GM103499 DRP to YS); the AHA (Grant-in-Aid, 15GRANT25710305 to YS) and an Award from the American Heart Association and the Lawrence J. and Florence A. DeGeorge Charitable Trust (YS). JGS was supported by 2016 MUSC Summer Undergraduate Research Program

(SURP). The contents are solely the responsibility of the authors and do not necessarily represent the official views of the NIH and AHA.

References

Abdelwahid E, Rice D, Pelliniemi LJ, Jokinen E. Overlapping and differential localization of BMP-2, BMP-4, Msx-2 and apoptosis in the endocardial cushion and adjacent tissues of the developing mouse heart. Cell Tissue Res. 2001; 305:67–78. [PubMed: 11512673]

Aikawa E, Whittaker P, Farber M, Mendleson K, Padera RF, Aikawa M, Schoen FJ. Human semilunar cardiac valve remodeling by activated cells from fetus to adult. Circulation. 2006; 113:1344–1352. [PubMed: 16534030]

Anderson RH, Spicer DE, Brown NA, Mohun TJ. The development of Septation in the four-chambered heart. Anat Rec. 2014; 297:1414–1429.

Armstrong EJ, Bishoff J. Heart valve development: endothelial cell signaling and differentiation. Circ Res. 2004; 95:459–470. [PubMed: 15345668]

Bai Y, Wang J, Morikawa Y, Bonilla-Claudio M, Klysik E, Martin JF. Bmp signaling represses Vegfa to promote outflow tract cushion development. Development. 2013; 140:3395–3402. [PubMed: 23863481]

Briggs LE, Phelps AL, Brown E, Kakarla J, Anderson RH, van den Hoff MJB, Wessels A. Expression of the BMP receptor Alk3 in the second heart field is essential for development of the dorsal mesenchymal protrusion and atrioventricular septation. Circ Res. 2013; 112:1420–1432. [PubMed: 23584254]

Burns T, Yang Y, Hiriart E, Wessels A. The dorsal mesenchymal protrusion and the pathogenesis of atrioventricular septal defects. J Cardiovasc Dev Dis. 2016; 3:29.doi: 10.3390/jcdd3030029 [PubMed: 28133602]

Cai J, Pardali E, Sanchez-Duffhues G, ten Dijke P. BMP signaling in vascular diseases. FEBS Lett. 2012; 586:1993–2002. [PubMed: 22710160]

Camenisch TD, Spicer AP, Brehm-Gibson T, Biesterfeldt J, Augustine ML, Calabro A Jr, Kubalak S, Klewer SE, McDonald JA. Disruption of hyaluronan synthase-2 abrogates normal cardiac morphogenesis and hyaluronan-mediated transformation of epithelium to mesenchyme. J Clin Invest. 2000; 106:349–360. [PubMed: 10930438]

Camenisch TD, Schroeder JA, Bradley J, Klewer SE, McDonald JA. Heart-valve mesenchyme formation is dependent on hyaluronan-augmented activation of ErbB2-ErbB3 receptors. Nat Med. 2002; 8:850–855. [PubMed: 12134143]

Chakraborty S, Cheek J, Sakthivel B, Arnow BJ, Yutzey KE. Shared gene expression profiles in developing heart valves and osteoblast progenitor cells. Physiol Genomics. 2008; 35:75–85. [PubMed: 18612084]

Chakraborty S, Combs MD, Yutzey KE. Transcriptional regulation of heart valve progenitor cells. Pediatr Cardiol. 2010; 31:414–421. [PubMed: 20039031]

Combs MD, Yutzey KE. Heart valve development. Regulatory networks in development and disease. Circ Res. 2009; 105:408–421. [PubMed: 19713546]

de Vlaming A, Sauls K, Hajdu Z, Visconti RP, Mehesz AN, Levine RA, Slaugenhaupt SA, Hagège A, Chester AH, Markwald RR, Norris RA. Atrioventricular valve development: new perspectives on an old theme. Differentiation. 2012; 84:103–116. [PubMed: 22579502]

Desgrosellier JS, Mundell NA, McDonnell MA, Moses HL, Barnett JV. Activin receptor-like kinase 2 and Smad6 regulate epithelial-mesenchymal transformation during cardiac valve formation. Dev Biol. 2005; 280:201–210. [PubMed: 15766759]

Dupuis LE, McCulloch DR, McGarity JD, Bahan A, Wessels A, Weber D, Diminich AM, Nelson CM, Apte SS, Kern CB. Altered versican cleavage in ADAMTS5 deficient mice; a novel etiology of myxomatous valve disease. Dev Biol. 2011; 357:152–164. [PubMed: 21749862]

Eisenberg L, Markwald RR. Molecular regulation of atrioventricular valvuloseptal morphogenesis. Circ Res. 1995; 77:1–6. [PubMed: 7788867]

Garside VC, Cullum R, Alder O, Lu DY, Werff RV, Bilenky M, Zhao Y, Jones SJM, Marra MA, Underhill TM, Hoodless PA. Sox9 modulates the expression of key transcription factors required for heart valve development. Development. 2015; 142:4340–4350. [PubMed: 26525672]

Goldman EC, Donley N, Christian JL. Genetic interaction between *Bmp2* and *Bmp4* reveals shared functions during multiple aspects of mouse organogenesis. Mech Dev. 2009; 126:117–127. [PubMed: 19116164]

Gomez-Stallons MV, Wirrig-Schwendeman EE, Hassel KR, Conway SJ, Yutzey KE. Bone morphogenetic protein signaling is required for aortic calcification. Arterioscler Thromb Vasc Biol. 2016; 36:1398–1405. [PubMed: 27199449]

Harikrishnan K, Cooley MA, Sugi Y, Barth JL, Rasmussen LM, Kern CB, Argraves KM, Argraves WS. Fibulin-1 suppresses endothelial to mesenchymal transition in the proximal outflow tract. Mech Dev. 2015; 136:123–32. [PubMed: 25575930]

Hinton RB, Lincoln J, Deutsch GH, Osinska H, Manning PB, Benson DW, Yutzey KE. Extracellular matrix remodeling and organization in developing and diseased aortic valves. Circ Res. 2006; 98:1431–1438. [PubMed: 16645142]

Hinton RB, Yutzey KE. Heart valve structure and function in development and disease. Annu Rev Physiol. 2011; 73:29–46. [PubMed: 20809794]

Inai K, Norris RA, Hoffman S, Markwald RR, Sugi Y. BMP-2 induces cell migration and periostin expression during atrioventricular valvulogenesis. Dev Biol. 2008; 315:383–396. [PubMed: 18261719]

Inai K, Burnside JL, Hoffman S, Toole BP, Sugi Y. BMP-2 induces versican and hyaluronan that contribute to post-EMT AV cushion cell migration. PLoS ONE. 2013; 8(10):e77593.doi: 10.137/journal.pone.0077593 [PubMed: 24147033]

Jiao K, Kulessa H, Tompkins K, Zhou Y, Batts L, Baldwin HS, Hogan BL. An essential role of BMP4 in the atrioventricular septation of the mouse heart. Genes Dev. 2003; 17:2362–2367. [PubMed: 12975322]

Lee MP, Yutzey KE. Twist1 directly regulates genes that promote cell proliferation and migration in developing heart valves. PLoS One. 2011; 6:e29758.doi: 10.1371/journal.pone.0029758 [PubMed: 22242143]

Levine RA, Hagége AA, Judge DP, Padala M, Dal-Bianco JP, Aikawa E, Beaudoin J, Bischoff J, Bouatia-Naji N, Bruneval P, Butcher JT, Carpentier A, Chaput M, Chester AH, Clusel C, Delling FN, Dietz HC, Dina C, Durst R, Fernandez-Friera L, Handschumacher MD, Jensen MO, Jeunemaitre XP, Le Marec H, Le Tourneau T, Markwald RR, Mérot J, Messas E, Milan DP, Neri T, Norris RA, Peal D, Perrocheau M, Probst V, Pucéat M, Rosenthal N, Solis J, Schott JJ, Schwammenthal E, Slaugenhaupt SA, Song JK, Yacoub MH. Leducq Mitral Transatlantic Network. Mitral valve disease--morphology and mechanisms. Nat Rev Cardiol. 2015; 12:689–710. [PubMed: 26483167]

Lincoln J, Garg V. Etiology of valvular heart disease-genetic and developmental origins. Circ J. 2014; 78:1801–1807. [PubMed: 24998280]

Lincoln J, Alfieri CM, Yutzey KE. BMP and FGF regulatory pathways control cell lineage diversification of heart valve precursor cells. Dev Biol. 2006a; 292:290–302.

Lincoln J, Florer JB, Deutsch GH, Wenstrup RJ, Yutzey KE. ColVa1 and ColXIa1 are required for myocardial morphogenesis and heart valve development. Dev Dyn 2006b. 2006b; 235:3295–3305.

Lincoln J, Kist R, Scherer G, Yutzey KE. Sox9 is required for precursor cell expansion and extracellular matrix organization during mouse heart valve development. Dev Biol. 2007; 305:120–132. [PubMed: 17350610]

Lindsley A, Snider P, Zhou H, Rogers R, Wang J, Olaopa M, Kruzynska-Frejtag A, Koushik SV, Lilly B, Burch JB, Firulli AB, Conway SJ. Identification and characterization of a novel Schwann and outflow tract endocardial cushion lineage-restricted periostin enhancer. Dev Biol. 2007; 307:340–55. [PubMed: 17540359]

Lockhart MM, Boukens BJD, Phelps AL, Brown CLM, Toomer KA, Burns TA, Mukherjee R, Norris RA, Trusk TC, van den Hoff MJB, Wessels A. Alk3 mediated Bmp signaling controls the contribution of epicardially derived cells to the tissues of the atrioventricular junction. Dev Biol. 2014; 396:8–18. [PubMed: 25300579]

Loffredo CA. Epidemiology of cardiovascular malformations: prevalence and risk factors. Am J Med Genet. 2000; 97:319–325. [PubMed: 11376444]

Luna-Zurita L, Prados B, Grego-Bessa J, Luxán G, del Monte G, Benguría A, Adams RH, Pérez-Pomares JM, de la Pompa JL. Integration of a Notch-dependent mesenchymal gene program and Bmp2-driven cell invasiveness regulates murine cardiac valve formation. J Clin Invest. 2010; 120:3493–3507. [PubMed: 20890042]

Ma L, Martin JF. Generation of a conditional null allele. Genesis. 2005; 42:203–206. [PubMed: 15986484]

Ma L, Lu MF, Schwartz RJ, Martin JF. Bmp2 is essential for cardiac cushion epithelial-mesenchymal transition and myocardial patterning. Development. 2005; 132:5601–5611. [PubMed: 16314491]

McCarthy K, Ho S, Anderson R. Ventricular septal defects: morphology of the doubly committed juxtaarterial and muscular variants. Images Paediatr Cardiol. 2000; 2:5–23. [PubMed: 22368583]

McCulley DJ, Kang JO, Martin JF, Black BL. BMP4 is required in the anterior heart field and its derivatives for endocardial cushion remodeling, outflow tract septation, and semilunar valve development. Dev Dyn. 2008; 237:3200–3209. [PubMed: 18924235]

Miyazono K, Kamiya Y, Morikawa M. Bone morphogenetic protein receptors and signal transduction. J Biochem. 2010; 147:35–51. [PubMed: 19762341]

Morrell NW, Bloch DB, ten Dijke P, Goumans MJTH, Hata A, Smith J, Yu PB, Bloch ED. Targeting BMP signaling in cardiovascular disease and anaemia. Nat Rev Cardiol. 2016; 13:106–120. [PubMed: 26461965]

Muzumdar MD, Tasic B, Miyamichi K, Li L, Luo LQ. A global double-fluorescent cre reporter mouse. Genesis. 2007; 45:593–605. [PubMed: 17868096]

Niessen K, Fu YX, Chang L, Hoodless PA, McFadden D, Karsan A. Slug is a direct Notch target required for initiation of cardiac cushion cellularization. J Cell Biol. 2008; 182:315–325. [PubMed: 18663143]

Norris RA, Moreno-Rodriguez RA, Sugi Y, Hoffman S, Amos J, Hart MM, Potts JD, Goodwin RL, Markwald RR. Periostin regulates atrioventricular valve maturation. Dev Biol. 2008; 316:200–213. [PubMed: 18313657]

Park C, Lavine K, Mishina Y, Deng CX, Ornitz DM, Choi K. Bone morphogenetic protein receptor 1A signaling is dispensable for hematopoietic development but essential for vessel and atrioventricular endocardial cushion formation. Development. 2006; 133:3473–3484. [PubMed: 16887829]

Peacock JD, Huk DJ, Ediriweera HN, Lincoln J. Sox9 transcriptionally represses Spp1 to prevent matrix mineralization in maturing heart valves and chondrocytes. PLoS One. 2011; 6(10):e26769.doi: 10.1371/journal.pone.0026769 [PubMed: 22046352]

Peacock JD, Lu Y, Koch M, Kadler KE, Lincoln J. Temporal and spatial expression of collagens during murine atrioventricular heart valve development and maintenance. Dev Dyn. 2008; 237:3051–3058. [PubMed: 18816857]

Peacock JD, Levay AK, Gillaspie DB, Tao G, Lincoln J. Reduced Sox9 function promotes heart valve calcification phenotype in vivo. Circ Res. 2010; 106:712–719. [PubMed: 20056916]

Person AD, Klewer SE, Runyan RB. Cell Biology of cardiac cushion development. Int Rev Cytol. 2005; 243:287–335. [PubMed: 15797462]

Richter A, Valdimarsdottir L, Hrafnkelsdottir HE, Runarsson JF, Omarsdottir AR, Oostwaard DWV, Mummery Cg, Valdimarsdottir G. BMP4 promotes EMT and mesodermal commitment in human embryonic stem cells via SLUG and MSX2. Stem Cells. 2014; 32:636–648. DOI: 10.1002/stem.1592 [PubMed: 24549638]

Rivera-Feliciano J, Tabin CJ. Bpm2 instructs cardiac progenitors to form the heart-valve-inducing field. Dev Biol. 2006; 295:580–588. [PubMed: 16730346]

Shelton EL, Yutzey KE. Twist function in endocardial cushion cell proliferation, migration, and differentiation during heart valve development. Dev Biol. 2008; 317:282–295. [PubMed: 18353304]

Singh AP, Castranio T, Scott G, Guo D, Harris MA, Ray M, Harris SE, Mishina Y. Influences of reduced expression of maternal bone morphogenetic protein 2 on mouse embryonic development. Sex Dev. 2008; 2:134–141. [PubMed: 18769073]

Snarr BS, Wirrig EE, Phelps AL, Trusk TC, Wessels A. A spatiotemporal evaluation of the contribution of the dorsal mesenchymal protrusion to cardiac development. Dev Dyn. 2007; 236:1287–1294. [PubMed: 17265457]

Snarr BS, Kern CB, Wessels A. Origin and fate of cardiac mesenchyme. Dev Dyn. 2008; 237:2804–2819. [PubMed: 18816864]

Song L, Faessler R, Mishina Y, Jiao K, Baldwin HS. Essential function of *Alk3* during AV cushion morphogenesis in mouse embryonic hearts. Dev Biol. 2007; 301:271–286.

Soriano P. Generalized lacZ expression with the ROSA26 Cre reporter strain. Nat Genet. 1999; 21(1): 70–1. [PubMed: 9916792]

Sugi Y, Yamamura H, Okagawa H, Markwald RR. Bone morphogenetic protein-2 can mediate myocardial regulation of atrioventricular cushion mesenchymal cell formation in mice. Dev Bio. 2004; 269:505–518. [PubMed: 15110716]

Sugi Y, Kern MJ, Markwald RR, Burnside JL. Periostin Expression is altered in aortic valves in Smad6 mutant mice. J Neonatal Biol. 2012; 1 pii: 4692.

Sugi, Y., Zhou, B., Inai, K., Mishina, Y., Burnside, JL. The role of cell autonomous signaling by BMP in endocardial cushion cells in AV valvuloseptal morphogenesis. Etiology and Morphogenesis of Congenital Heart Disease. In: Nakanishi, T., et al., editors. In Etiology and Morphogenesis of Congenital Heart Disease. 2016. p. 171-173.

Tasaka H, Krug EL, Markwald RR. Origin of the pulmonary venous orifice in the mouse and its relation to the morphogenesis of the sinus venosus, extracardiac mesenchyme (spina Vestibuli), and Atrium. Anat Rec. 1996; 246:107–113. [PubMed: 8876829]

Thomas PS, Rajderkar S, Lane J, Mishina Y, Kaartinen V. AcvR1-mediated BMP signaling in second heart field is required for arterial pole development: Implications for myocardial differentiation and regional identity. Dev Biol. 2014; 390:191–207. [PubMed: 24680892]

Toole BP, Yu Q, Underhill GB. Hyaluronan and hyaluronan-binding proteins. Probes for specific detection. Methods Mol Biol. 2001; 171:479–485. [PubMed: 11450261]

Uchimura T, Komatsu Y, Tanaka M, McCann KL, Mishina M. *Bmp2* and *Bmp4* genetically interact to support multiple aspects of mouse development including functional heart development. Genesis. 2009; 47:374–384. [PubMed: 19391114]

Wang J, Greene SB, Martin JF. BMP signaling in congenital heart disease: new developments and future directions. Birth Defects Res A Clin Mol Teratol. 2011; 91:441–448. [PubMed: 21384533]

Wang J, Sridurongrit S, Dudas M, Thomas P, Nagy A, Schneider MD, Epstein JA, Kaartinen V. Atrioventricular cushion transformation is mediated by ALK2 in the developing mouse heart. Dev Biol. 2005; 286:299–310. [PubMed: 16140292]

Wang Y, Wu B, Chamberlain A, Lui W, Koirala P, Susztak K, Klein D, Taylor V, Zhou B. Endocardial to myocardial Notch-Wnt-Bmp Axis regulates early heart valve development. PLoS ONE. 2013; 8(4):e60244.doi: 10.1371/journal.pone.0060244 [PubMed: 23560082]

Webb S, Brown NA, Anderson RH. Formation of the atrioventricular septal structures in the normal mouse. Circ Res. 1998; 82:645–656. [PubMed: 9546373]

Wu B, Zhang Z, Lui W, Chen X, Wang Y, Chamberlain AA, Moreno-Rodriguez RA, Markwald RR, O'Rourke BP, Sharp DJ, Zhen D, Lenz J, Baldwin HS, Chang CP, Zhou B. Endocardial cells form the coronary arteries by angiogenesis through myocardial-endocardial VEGF signaling. Cell. 2012; 151:1083–1096. [PubMed: 23178125]

Yamamura H, Zhang M, Markwald RR, Mjaatvedt CH. A heart segmental defect in the anterior-posterior axis of a transgenic mutant mouse. Dev Biol. 1997; 186:58–72. [PubMed: 9188753]

Yang W, Guo D, Harris MA, Cui Y, Gluhak-Heinrich J, Wu J, Chen X-D, Skinner C, Nyman JS, Edwards JR, Mundy GR, Lichtler A, Kream BE, Rowe DW, Kalajzic I, David V, Quarles DL, Villareal D, Scott G, Ray M, Liu S, Martin JF, Mishina Y, Harris SE. *Bmp2* in osteoblasts of periostium and trabecular bone links bone formation to vascularization and mesenchymal stem cells. J Cell Sci. 2013; 126:4085–4098. [PubMed: 23843612]

Zhang H, Bradley A. Mice deficient for BMP2 are nonviable and have defects in amnion/chorion and cardiac development. Development. 1996; 122:2977–2986. [PubMed: 8898212]

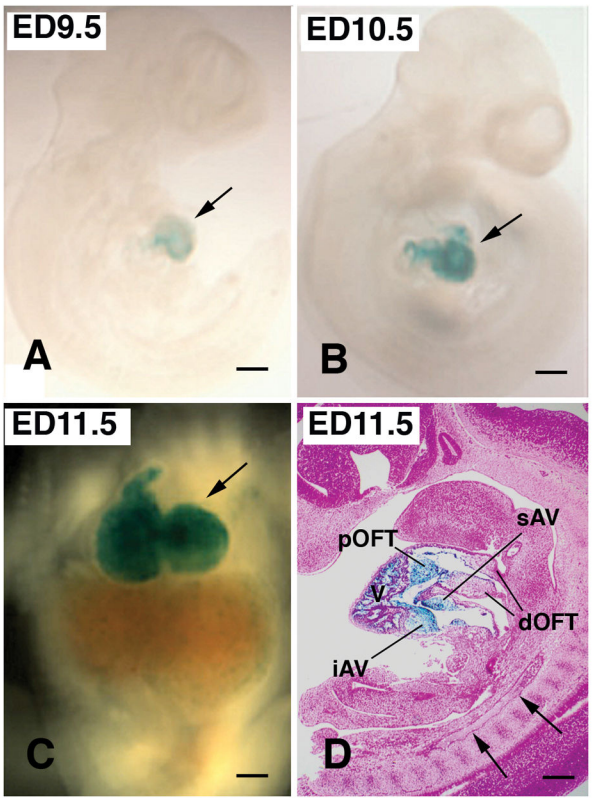

Fig. 1.

Nfatc1^{Cre}*; R26R* mouse embryos stained with X-gal show Cre-mediated recombination exclusively in the heart during early heart development (A–D). Whole mount preparation of mouse embryos from ED9.5 to ED11.5 (A–C) shows Cre-mediated recombination exclusively in the heart (blue color, arrows in A–C). Cre-mediated recombination is restricted to endocardial cells and their transformed progeny mesenchymal cells at ED 11.5 (D). There is no detectable recombination in other vasculature (arrows in D). Note that proximal OFT (pOFT) as well as superior and inferior AV (sAV and iAV) cushion mesenchymal cells are all Lac-Z positive (blue color), indicating that these mesenchymal cells are derived from the Nfatc1-positive endocardium. In contrast, mesenchymal cells in the distal outflow tract (dOFT) are not LacZ-positive, which indicates that these mesenchymal cells do not have endocardial origin. V, ventricle. Scale bars=200μm.

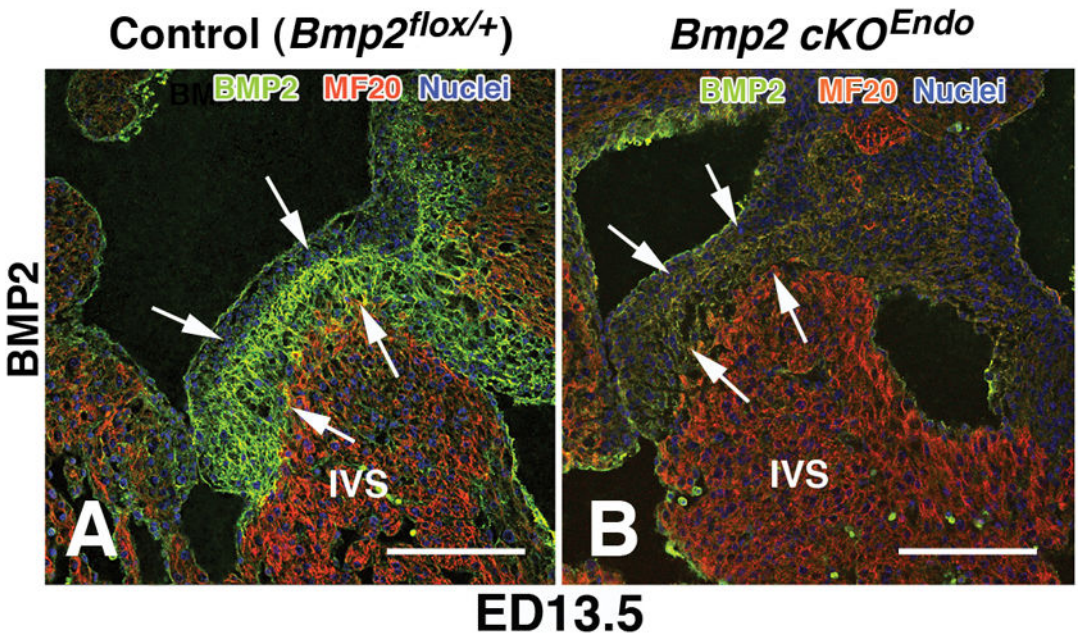

Fig. 2.

Reduction of BMP2 in AV endocardial cushions is detected in a *Bmp2 cKO*^{Endo} mouse embryo at ED13.5. BMP2 is immunohistochemically localized in the AV endocardial cushions in a *Bmp2*$^{fx/+}$ control mouse embryo at ED13.5 (arrows in A). Significant reduction of BMP2 is detected in the AV endocardial cushions in a littermate *Bmp2 cKO*^{Endo} mouse AV cushions (arrows in B) when compared to the control. IVS, interventricular septum. Scale bars=200μm.

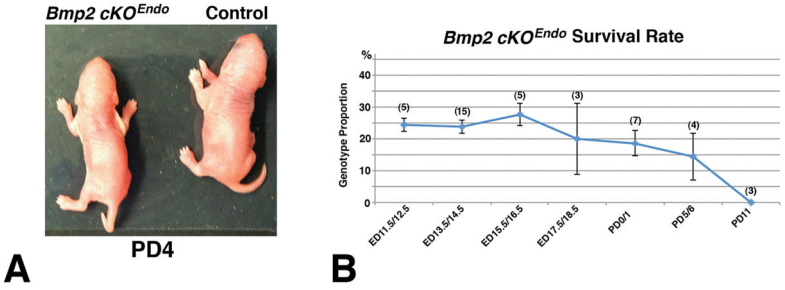

Fig. 3.

Bmp2 cKO^{Endo} mice survive until birth but die shortly after birth. Some of the most affected one die within the first day after birth. Other *Bmp2* cKO^{Endo} mice that exhibit milder phenotypes start showing loss of body weight and mobility (A) and die within several days after birth. *Bmp2 cKO*^{Endo} mouse survival rate is around 25%, as predicted by Mendelian frequencies until birth, but drops sharply after birth (B). Error bars represent standard error of the mean (SEM). The number in parenthesis indicates the number of litters that were evaluated.

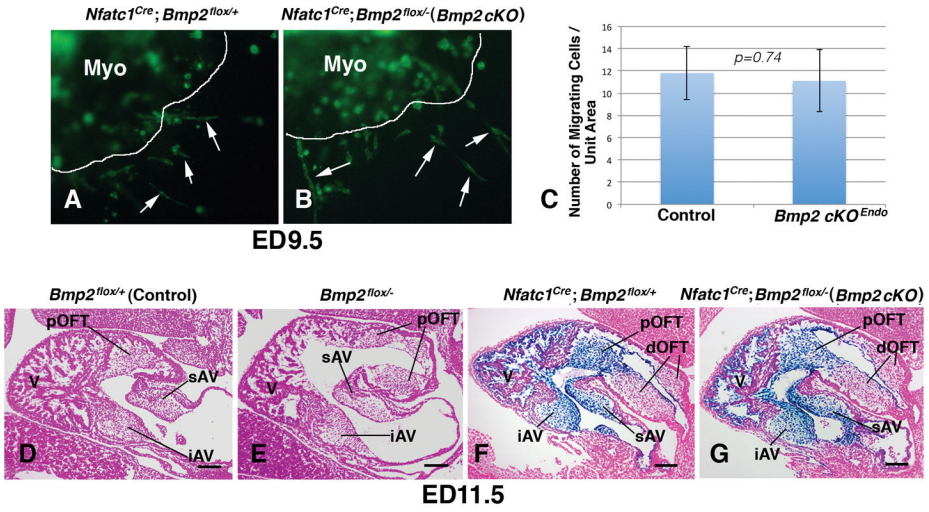

Fig. 4.

Deletion of *Bmp2* in the endocardial lineage does not reduce or delay AV cushion formation. A and B show migration of endocardial cushion mesenchymal cells from AV explants of *Nfatc1* ^{Cre}*; Bmp2* $^{fx/+}$*; ROSA26*^{mG} (A) and *Nfatc1* ^{Cre}*; Bmp2* $^{fx/-}$*; ROSA26*^{mG} (*Bmp2 cKO*^{Endo}) (B) mouse embryos. Endocardial cells and endocardial progeny mesenchymal cells that express *Nfatc1*^{Cre} are marked by green fluorescent protein (GFP) (green color). A and B show AV endocardial cushions with associated AV myocardium (Myo, GFP-negative) cultured on collagen gels from ED9.5 littermate mouse embryos. Arrows indicate migrating endocardial cushion mesenchymal cells. C shows a histogram showing the numbers of mesenchymal cells migrated out from the explants per unit area, indicating that there is no significant difference ($p=0.74$). D–G are sagittal sections from littermates, *Bmp2*$^{fx/+}$ (control) (D), *Bmp2*$^{fx/-}$ (*Bmp2* heterozygous) (E), *Nfatc1*^{Cre}*; Bmp2*$^{fx/+}$*; R26R* (*Bmp2* endocardial conditional heterozygous) (F) and *Nfatc1*^{Cre}*; Bmp2*$^{fx/-}$*; R26R* (*Bmp2 cKO*^{Endo}) (G) mouse embryos at ED11.5. AV and pOFT endocardial cushions are formed normally in a *Bmp2* cKO^{Endo} mouse heart (G) when compared to a control (D). *Bmp2* Heterozygous (E) and conditional heterozygous (F) embryos do not exhibit reduction of endocardial cushion formation, either. Sections are stained with LacZ and counter stained with Eosin. A, atrium; V, ventricle; iAV, inferior AV cushion; sAV, superior AV cushion; pOFT, proximal outflow tract cushion. Scale bars=100μm.

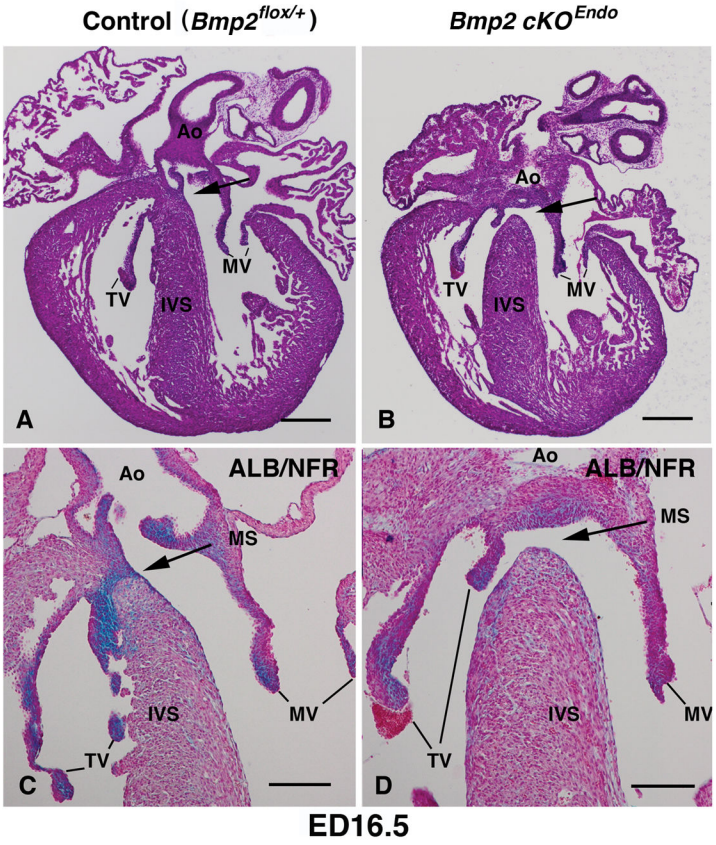

Fig. 5.

Bmp2 cKO^{Endo} mouse embryos consistently exhibit (peri)-membranous ventricular septal defects (VSD) at ED16.5 with nearly complete penetrance (92%, n=13). *Bmp2*$^{fx/+}$ (control) (A and C) and *Nfatc1*^{Cre}*; BMP2*$^{fx/-}$ (*Bmp2 cKO*^{Endo}) (B and D). A and B are stained with hematoxylin and eosin (H &E) and C and D are stained with Alcian Blue (ALB) and counter stained with Nuclear Fast Red (NFR). Arrows show membranous ventricular septum in A and C and membranous VSD in B and D. C and D are higher magnification views. Ao, aorta, TV; tricuspid valves; MV, mitral valves; IVS, interventricular septum; MS, membranous septum. Scale bars in A and B=200μm. Scale bars in C and D=100μm.

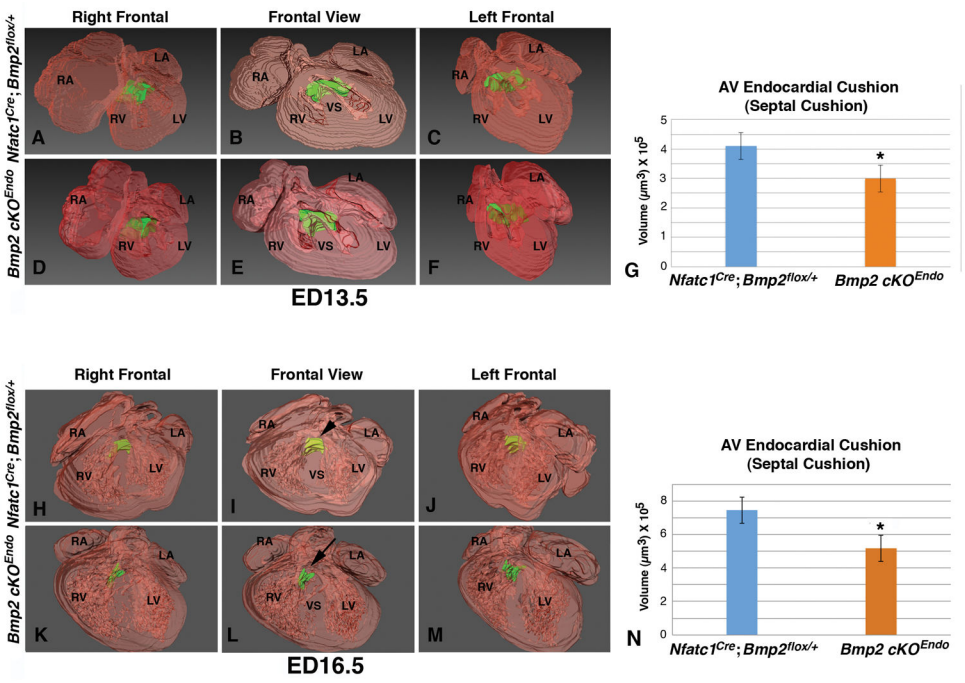

Fig. 6.

Bmp2 cKO^{Endo} mouse embryos exhibit decreased AV septal cushion size at ED13.5 and ED16.5. Three dimensional (3D) reconstructions were generated from frontal sections of *Nfatc1*^{Cre}; *Bmp2*$^{flox/+}$; *R26R* (A–C) and *Nfatc1*^{Cre}; *Bmp2*$^{flox/-}$; *R26R* (*Bmp2 cKO*^{Endo})(D–F) mouse hearts at ED13.5 and *Nfatc1*^{Cre}*; BMP2*$^{flox/+}$; *R26R* (H–J) and *Nfatc1*^{Cre}; *BMP2*$^{flox/-}$; *R26R* (*Bmp2 cKO*^{Endo}) (K–M) hearts at ED16.5. Amira 3D volumetric analysis reveals a significant decrease in size of septal AV cushions at ED13.5 (asterisk in G, $p<0.05$) as well as at ED16.5 (asterisk in N, $p<0.05$). An arrowhead in I indicates membranous ventricular septum (VS) in a control and an arrow in L indicates partial loss of membranous ventricular septum in a *Bmp2 cKO*^{Endo} mouse embryo.

LA, left atrium; LV, left ventricle; RA, right atrium; RV, right ventricle; VS, ventricular septum. Green collar indicates septal AV cushions. Error bars represent SEM (n=5).

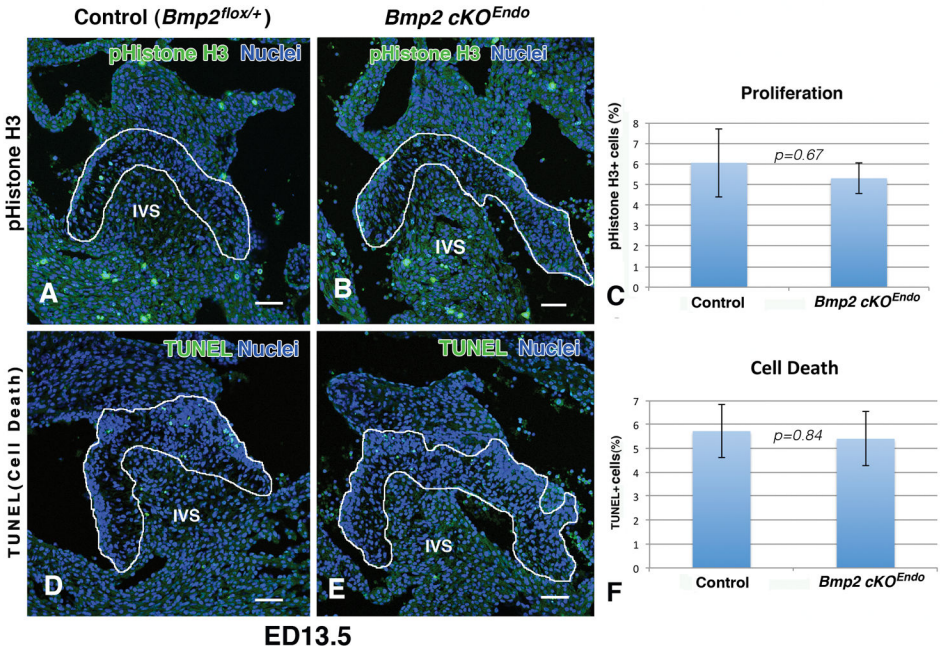

Fig. 7.

Bmp2 cKO^{Endo} mouse embryos do not exhibit a significant reduction of proliferation or an increase of cell death in AV septal cushions at ED13.5. Phospho-histone H3 (pHistone H3) immunohistochemistry was performed to detect proliferation ratio for AV endocardial cushions in control (*Bmp2*$^{fx/+}$) (A) and *Bmp2 cKO*^{Endo} (B) mouse embryos. All nuclei were stained with TO-PRO-3 (blue). pHistone H3 staining does not show significant differences between control and *Bmp2 cKO*^{Endo} (C) (p=0.67). TUNEL assay was performed to detect cell death for AV endocardial cushions in control (*BMP2* $^{fx/+}$) (D) and *Bmp2 cKO*^{Endo} (E) mouse embryos. There is no significant difference between control and *Bmp2 cKO*^{Endo} (F) (p=0.84). White line marks AV endocardial cushions. IVS, interventricular septum. Error bars represent SEM (n=5). Scale bars=100μm.

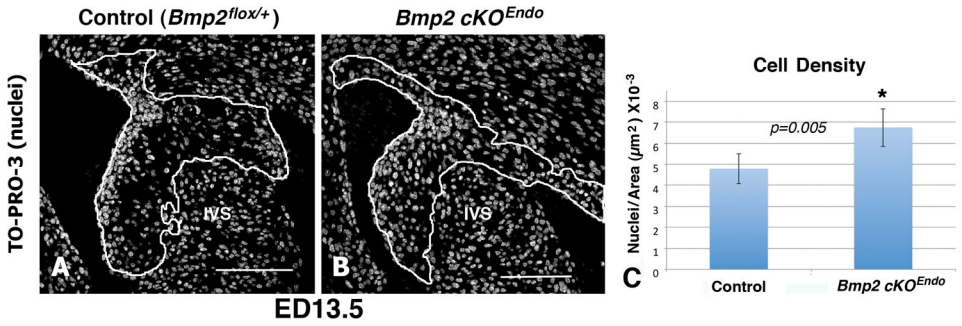

Fig. 8.

Bmp2 cKO^{Endo} mouse embryos show a significant increase in cell density in AV septal cushions at ED13.5. All nuclei were stained with TO-PRO-3 in AV septal cushions at ED13.5 in control (*Bmp2*$^{fx/+}$) (A) and *Bmp2 cKO*^{Endo} (B) mouse embryos. White line marks AV endocardial cushions. IVS, interventricular septum. There is a significant increase (asterisk in C, $p<0.05$) in cell density of *Bmp2 cKO*^{Endo} mouse AV septal cushions as compared to controls (C), suggesting a decrease in intercellular space in *Bmp2 cKO*^{Endo} mouse AV septal cushions. IVS, interventricular septum. Error bars represent SEM (n=5). Scale bars=200μm.

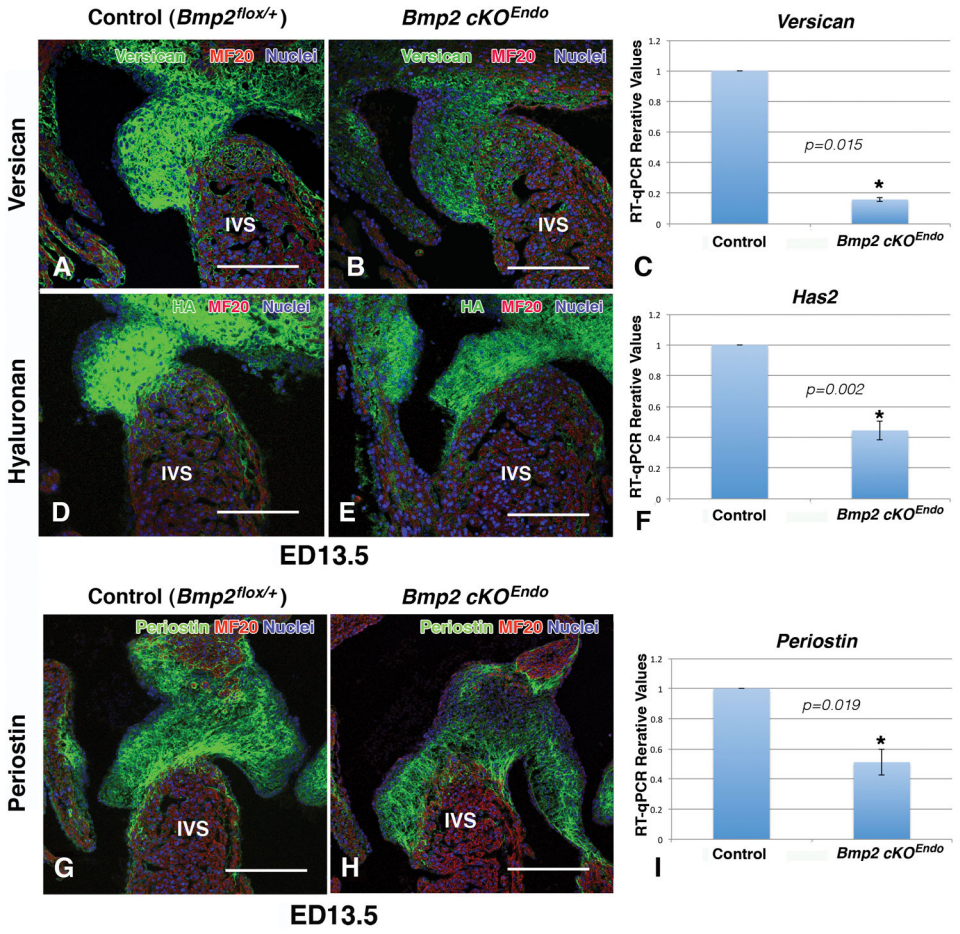

Fig. 9.

Bmp2 cKO^{Endo} mouse embryos show significant reductions in mRNA expression of proteoglycans, *versican* and *Has2,* and matricellular protein, *periostin* in the septal portion of the AV canal. Versican, hyaluronan and periostin are localized in the control (A, D and G) and *Bmp2 cKO*^{Endo} (B, E and H) septal AV cushions at ED13.5. mRNA expression of *versican* (C), *Has2* (F) and *periostin* (I) is significantly reduced in the *Bmp2 cKO*^{Endo} mouse AV canals at ED13.5 (asterisks, $p<0.05$) as compared to controls. IVS, interventricular septum. Error bars represent SEM (n=5). Scale bars=200μm.

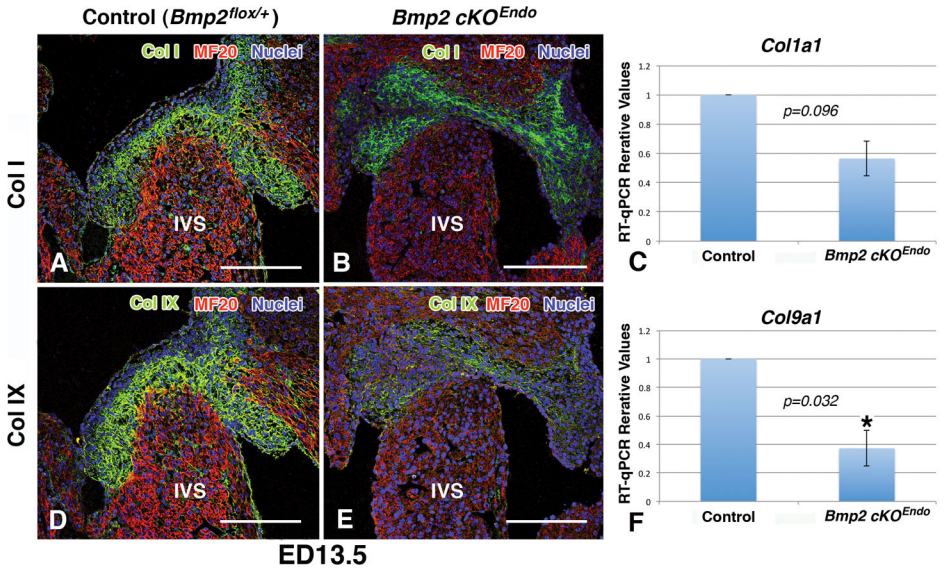

Fig. 10.

Bmp2 cKO^{Endo} mouse embryos show a significant reduction in mRNA expression of *Collagen 9a1* (*Col 9a1*) in the septal portion of the AV canal at ED13.5. Collagen I (Col I) and Col IX are expressed in control (A and D) and *Bmp2 cKO*^{Endo} (B and E) septal AV cushions at ED13.5. mRNA expression of *Col 1a1* (C) is slightly reduced but not significantly (p=0.096); however, *Col 9a1* (F) is significantly reduced (p=0.032) in the *Bmp2 cKO*^{Endo} mouse AV canals as compared to controls. IVS, interventricular septum. Error bars represent SEM (n=5). Scale bars=200μm.

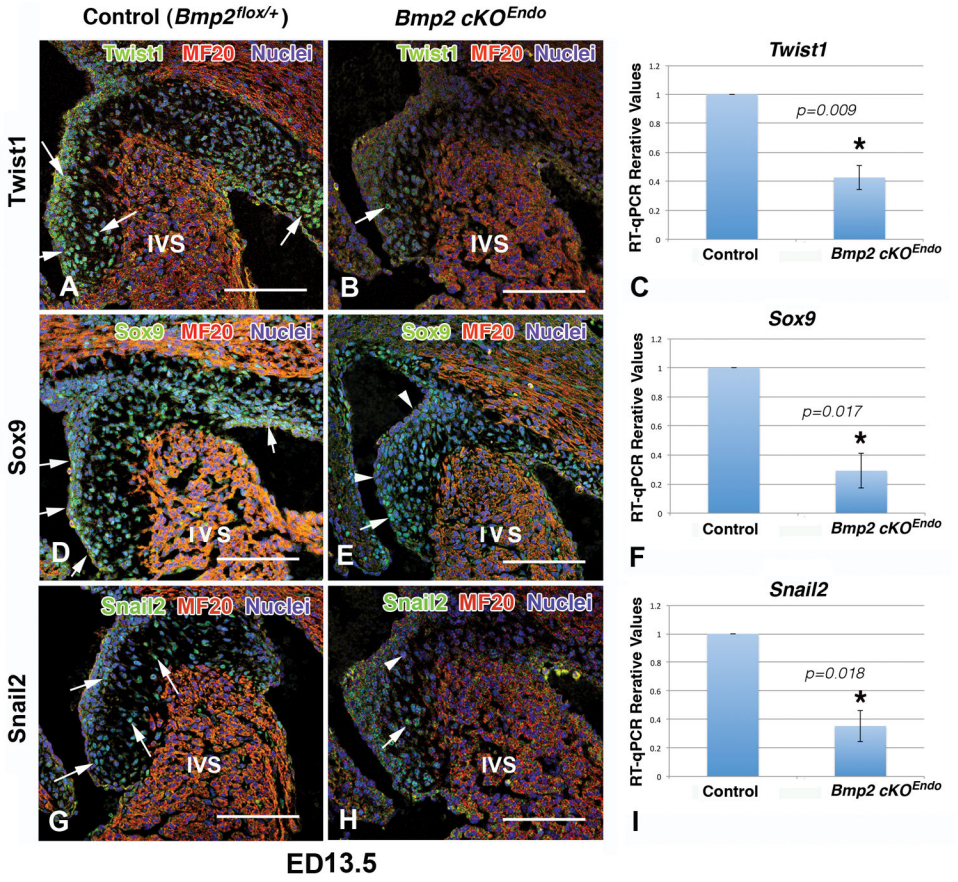

Fig. 11.

Bmp2 cKO^{Endo} mouse embryos exhibit significant reductions in mRNA expression of transcription factors, *Twist1*, *Sox9*, and *Snail2* in the septal portion of the AV canal at ED13.5. Twist1, Sox9 and Snail1 are expressed in the control (A, D and G) and *Bmp2 cKO*^{Endo} (B, E and H) septal AV cushions at ED13.5. mRNA expression of *Twist1* (C), *Sox9* (F) and *Snail2* (I) is significantly reduced (asterisks, $p<0.05$) in the *Bmp2 cKO*^{Endo} mouse AV canals as compared to controls. Error bars represent SEM (n=5). Scale bars=200μm.

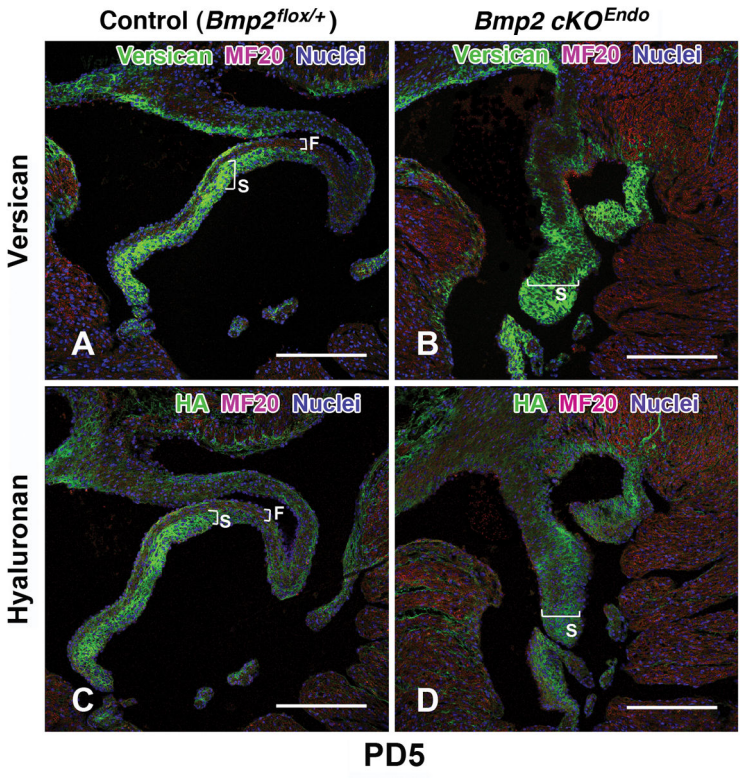

Fig. 12.

Immunohistochemical localization of versican (A, B), hyaluronan (C, D) in control (A, C) and *Bmp2 cKO*^{Endo} (B, D) mouse mitral valves at postnatal day 5 (PD) 5. Versican (A) and hyaluronan (C) are intensely expressed in the spongiosa (S) in the control valves; however, *Bmp cKO*^{Endo} valves (B, D) exhibit loss of stratification and expansion of the spogiosa (B, D). Scale bars=200μm.

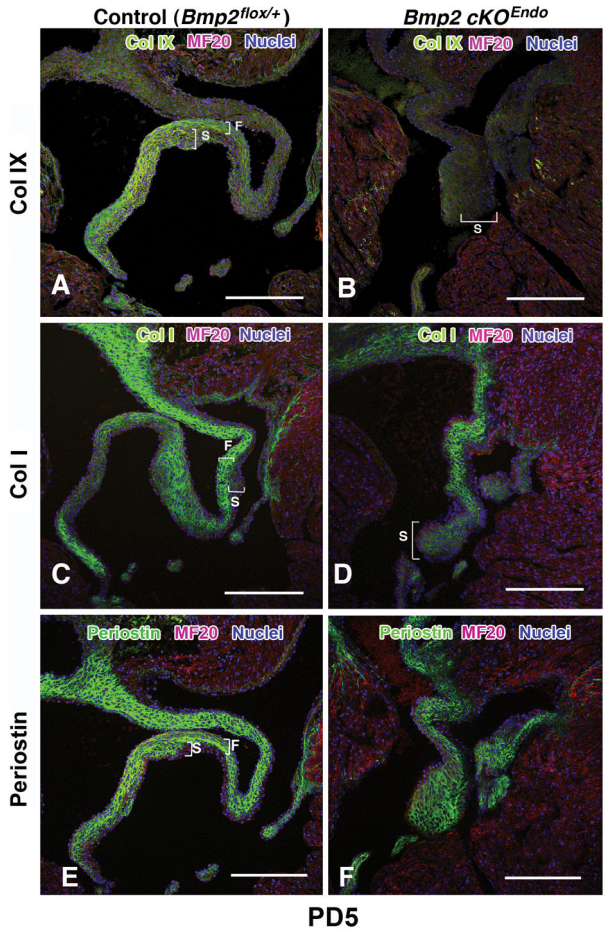

Fig. 13.

Immunohistochemical localization of Collagen IX (Col IX) (A, B), Collagen I (Col I) (C, D) and periostin (E, F) in control (A, C, E) and *Bmp2 cKO*^{Endo} (B, D, F) mouse mitral valves at PD5. Collagens are intensely expressed in the fibrosa (F) but not in the spongiosa (S) in the control valves (A, C); however, *Bmp cKO*^{Endo} valves (B, D) exhibit loss of stratification and expansion of the spogiosa (B, D). Periostin is deposited in the fibrosa in a pattern similar to that of collagen deposition in the control (E) but is entirely dispersed in the enlarged *Bmp2 cKO*^{Endo} mitral valve leaflets (F). Scale bars=200μm.

Table 1

Frequency of Genotypes Obtained and Timing of Lethality for *Bmp2 cKO^{Endo}*.

Stage (dpc)	*Nfatc1^{cre};Bmp2$^{flox/-}$* (*Bmp2 cKO^{Endo}*)	*Bmp2$^{fx/-}$*	*Nfatc1^{cre};Bmp2$^{flox/+}$*	*Bmp2$^{flox/+}$(Control)*	*Bmp2 cKO^{Endo}*
ED11.5/12.5	9	12	6	10	24.3%
ED13.5/14.5	37	36	44	39	23.7%
ED15.5/16.5	13	12	10	12	27.7%
ED17.5/18.5	5	6	7	7	20.0%
PD0/1/2	9	9	15	17	18.0%
PD5/6	2	3	4	5	14.3%
PD11	0	4	4	6	0.0%